AD-A089 266 CIVIL ENGINEERING LAB (NAVY) PORT HUENEME CA F/G 11/2
FIBERGLASS-REINFORCED RIGID POLYURETHANE EXPEDIENT PAVEMENT SUB--ETC(U)
MAY 80 P S SPRINGSTON
UNCLASSIFIED CEL-TN-1578 NL

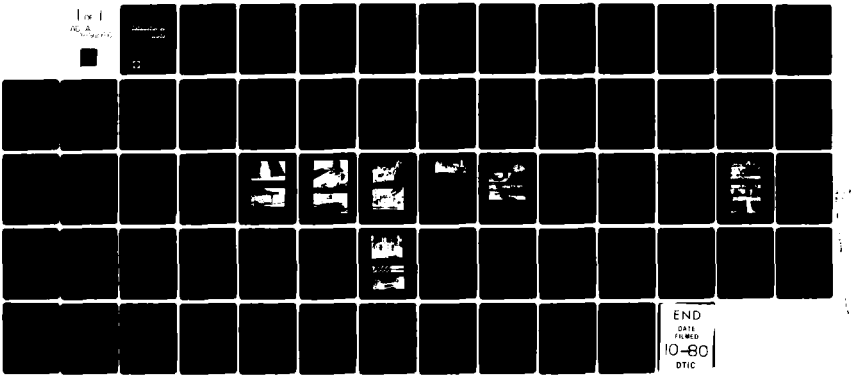

END
DATE FILMED
10-80
DTIC

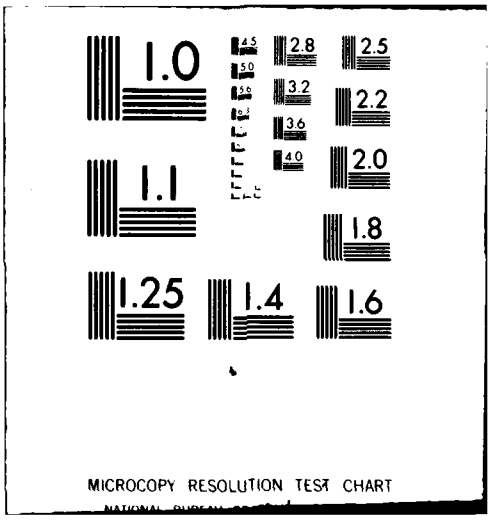
1.0
1.1
1.25
1.4
1.6
1.8
2.0
2.2
2.5
2.8
3.2
3.6
4.0
4.5
5.0
5.6
MICROCOPY RESOLUTION TEST CHART

LEVEL II

(12)

Technical Note

CEL

TN no. N-1578

title: FIBERGLASS-REINFORCED RIGID POLYURETHANE EXPEDIENT PAVEMENT SUBJECT TO SIMULATED F-4 AIRCRAFT TRAFFIC

author: P. S. Springston

date: May 1980

sponsor: Naval Facilities Engineering Command

program nos: YF53.536.091.01.003E

CIVIL ENGINEERING LABORATORY
NAVAL CONSTRUCTION BATTALION CENTER
Port Hueneme, California 93043

(14) CEL-TN-1578

Unclassfied

SECURITY CLASSIFICATION OF THIS PAGE (When Data Entered)

REPORT DOCUMENTATION PAGE		READ INSTRUCTIONS BEFORE COMPLETING FORM
1. REPORT NUMBER TN-1578	2. GOVT ACCESSION NO. DN244122	3. RECIPIENT'S CATALOG NUMBER AD-A089 966
4. TITLE (and Subtitle) (4) FIBERGLASS-REINFORCED RIGID POLYURETHANE EXPEDIENT PAVEMENT SUBJECT TO SIMULATED F-4 AIRCRAFT TRAFFIC		5. TYPE OF REPORT & PERIOD COVERED Not final; FY 79 6. PERFORMING ORG. REPORT NUMBER
7. AUTHOR(s) (10) P. S. Springston		8. CONTRACT OR GRANT NUMBER(s) (9) Technical notes
9. PERFORMING ORGANIZATION NAME AND ADDRESS CIVIL ENGINEERING LABORATORY Naval Construction Battalion Center Port Hueneme, California 93043		10. PROGRAM ELEMENT, PROJECT, TASK AREA & WORK UNIT NUMBERS (11) YF53.536.091.01.003E; 62760N
11. CONTROLLING OFFICE NAME AND ADDRESS Naval Facilities Engineering Command Alexandria, Virginia 22332 (16)		12. REPORT DATE May 1980 (12) 64 13. NUMBER OF PAGES 63
14. MONITORING AGENCY NAME & ADDRESS(if different from Controlling Office) (17) YF53.536.01.1		15. SECURITY CLASS. (of this report) Unclassified 15a. DECLASSIFICATION/DOWNGRADING SCHEDULE

16. DISTRIBUTION STATEMENT (of this Report)

Approved for public release; distribution unlimited.

17. DISTRIBUTION STATEMENT (of the abstract entered in Block 20, if different from Report)

18. SUPPLEMENTARY NOTES

19. KEY WORDS (Continue on reverse side if necessary and identify by block number)

Soil surfacing, expedient airfield pavements, expeditionary airfields, fiberglass reinforced plastics, rigid polyurethane foam

20. ABSTRACT (Continue on reverse side if necessary and identify by block number)

A multipurpose expedient paving system is being developed to enable more rapid construction of expeditionary airfields by Marine Corps forces engaged in an amphibious landing. Previous research has resulted in a conceptual pavement, FIBERMAT, which consists of a facing of fiberglass-reinforced polyester resin (FRP) bonded to a core of fiberglass-reinforced rigid polyurethane foam. FIBERMAT has been subjected to a series of laboratory tests to define response to stress fatigue and environmental cycling. A similar

(continued)

DD FORM 1 JAN 73 1473 EDITION OF 1 NOV 65 IS OBSOLETE

Unclassified

SECURITY CLASSIFICATION OF THIS PAGE (When Data Entered)

Block 20. Continued

structural sandwich of FRP and rigid polyurethane foam has been tested and found to meet F-4 aircraft static load, tailhook impact, and engine exhaust blast requirements. This report documents the results of a traffic test conducted on a section of FIBERMAT having a 5-inch-thick fiberglass-reinforced foam core and a 1/4-inch-thick FRP facing. Distributed traffic was applied to the test secton with a load cart which simulated a main gear of an F-4 aircraft. The cart was equipped with a 30-7.7, 18-ply-rating tire inflated to 265 psi and loaded to 27,000 pounds. The first failure within the test section was recorded at 136 coverages (1,306 passes) of the load cart, and the entire test section was considered failed at 310 coverages (2,141 passes).

Library card

Civil Engineering Laboratory
FIBERGLASS-REINFORCED RIGID POLYURETHANE EXPEDIENT PAVEMENT SUBJECT TO SIMULATED F-4 AIRCRAFT TRAFFIC, by P. S. Springston
TN-1578 63 pp illus May 1980 Unclassified

A multipurpose expedient paving system is being developed to enable more rapid construction of expeditionary airfields by Marine Corps forces engaged in an amphibious landing. Previous research has resulted in a conceptual pavement, FIBERMAT, which consists of a facing of fiberglass-reinforced polyester resin (FRP) bonded to a core of fiberglass-reinforced rigid polyurethane foam. FIBERMAT has been subjected to a series of laboratory tests to define response to stress fatigue and environmental cycling. A similar structural sandwich of FRP and rigid polyurethane foam has been tested and found to meet F-4 aircraft static load, tailhook impact, and engine exhaust blast requirements. This report documents the results of a traffic test conducted on a section of FIBERMAT having a 5-inch-thick fiberglass-reinforced foam core and a 1/4-inch-thick FRP facing. Distributed traffic was applied to the test secton with a load cart which simulated a main gear of an F-4 aircraft. The cart was equipped with a 30-7.7, 18-ply-rating tire inflated to 265 psi and loaded to 27,000 pounds. The first failure within the test section was recorded at 136 coverages (1,306 passes) of the load cart, and the entire test section was considered failed at 310 coverages (2,141 passes).

CONTENTS

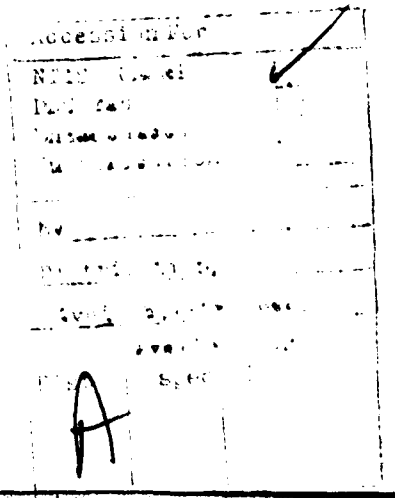

INTRODUCTION

Objective

The overall objective of the medium-duty airfield pavement project is to develop the technology necessary for Marine and Navy engineer units to have an improved capability of expediently constructing an airfield pavement in an Amphibious Objective Area (AOA). The pavement is to be characterized by (1) adaptation to specific soil strength and aircraft loads, (2) rapid field construction, (3) durability, and (4) minimal logistics burden. The current objective is to render an interim decision on the technical feasibility as related to trafficability and logistics of such an airfield pavement. This document presents the results of traffic testing of the pavement with simulated F-4 aircraft traffic at Tyndall AFB, Fla. with the assistance of the Air Force Engineering and Services Center (AFESC).

Background

The military has extensively developed and tested families of prefabricated mattings for use on tactical airfields. Such mattings have performed adequately, although they have proven to have several disadvantages, including: difficulty of bomb damage repair, infiltration of water through joints with subsequent deterioration of subgrade support, and inefficiency of design. Because mattings are designed and fabricated for "worst case" combinations of soil conditions and aircraft loadings, inefficiency results when the mattings are utilized on stronger subgrades or under lighter aircraft loadings than originally specified.

The Multipurpose Expedient Paving System (MEPS) would present the tactical engineer with an opportunity to quickly design and field-fabricate a pavement to realize economic advantage from a pavement designed for the various traffic areas, aircraft loadings, and soil conditions existent within an airfield. Additional logistic benefit would accrue from the expansion characteristics of the polyurethane foam core material - 1 ft^3 of transported fluid components expands to 3 to 4 ft^3 of rigid foam in the AOA. The pavement used in the MEPS is termed FIBERMAT.

FIBERMAT is a field-fabricated pavement consisting of a 2- to 5-inch-thick core of fiberglass-reinforced rigid (20 pcf) polyurethane foam with a bonded upper wearing surface of 1/8 or 1/4 inch of fiberglass-reinforced polyester resin (FRP). Previous research (Ref 1) led to (1) the establishment of required characteristics for the pavement and (2) the testing of FIBERMAT for resistance to load-induced fatigue and the effects of environmental cycling. Follow-on efforts focused on the prediction of ambient temperature effects and resulted in development of construction and expansion joints. Earlier research had produced a similar pavement - FOMAT, a structural sandwich consisting of a 2-inch core of unreinforced rigid (20 pcf) polyurethane with facings of 1/4-inch-thick FRP - which successfully withstood tests simulating jet aircraft engine heat and exhaust blast and tail hook impact (Ref 2). FOMAT did not withstand simulated F-4 traffic and could not be field-fabricated;

however, it lead to the FIBERMAT concept. The performance of FIBERMAT with respect to jet engine exhaust and tail hook impact is expected to be similar to that of FOMAT.

DEFINITION OF TERMS

For information and clarity, certain terms used in this report are defined as follows:

Test section: The prepared area, including the expedient pavement for test purposes.

Traffic lane: Area of the expedient pavement that is subjected to the rolling wheel load of the load cart.

Subgrade: The portion of the test section constructed with soil processed under controlled conditions to provide the desired bearing capacity and upon which the expedient pavement is placed.

CBR (California Bearing Ratio): A measure of the bearing capacity of the soil based upon its shearing resistance. CBR is calculated by dividing the unit load required to force a standardized piston into soil at a standardized rate by the unit load required to force the same piston at the same rate into a standard sample of crushed stone and multiplying by 100.

Deflection: Temporary bending of the surfacing under the static load from the test wheel of the load cart.

Transverse dishing: Permanent bending of the surfacing perpendicular to the direction of traffic.

Longitudinal dishing (with reference to the panel): Permanent bending of the surfacing parallel to the direction of traffic.

Direction of traffic: The direction in which the load cart travels on the test section. The direction of traffic is representative of actual landing directions with respect to construction joints.

Coverage: One application of the test wheel of the load cart over every point within the center 60 inches of the traffic lane.

Load cart: A specially constructed cart used in AFESC engineering tests for simulating aircraft taxiing operations.

Test wheel: The wheel on the load cart that supports the test load.

SUBGRADE PREPARATION

For the trafficability testing, a heavy clay (CH*) subgrade was used to represent a "worst case" soil that would be encountered in expedient airfield construction. A description of the test facility and the physical properties and mineralogical composition of the clay are contained

*Classification by the Uniform Soil Classification System (Ref 3).

in Appendix A. Removal of a previously tested pavement left the subgrade below the specified elevation for the lower pavement surface. Thus, a clay lift of approximately 6 to 8 inches was added to the test pit and then compacted and graded to bring the subgrade to within 5 inches of the surface of the surrounding concrete pavement. Moisture/density tests of the clay were conducted at depths ranging from 0 to 12 inches by AFESC and CEL personnel (Figure 1 and Table 1). In 27 tests the average dry density of the subgrade was 95.4 pcf at an average moisture content of 29.8% (by dry weight of soil). Eight CBR tests were performed in the laboratory on samples of Wewahitchka clay used in the subgrade. The moisture content of the clay used in the CBR tests ranged from 22.9 to 30.1% (by dry weight of soil). A plot of dry density versus CBR revealed a linear relationship with a coefficient of determination of 0.96 over the relatively narrow range of dry densities (Figure 2). Given the average dry density of the subgrade, and solving the linear equation of Figure 2 for CBR, yielded an average CBR value of 5.9% for the clay subgrade; thus, the clay subgrade was rated as having a CBR of 5.9%.

After final grading and soil testing were completed, the clay subgrade was instrumented in two locations (Figure 3) with soil strain gages. At each location, the strain gages - Bison soil strain sensors - were placed in a vertical stack with sensors in parallel and coaxial alignment with individual gages located at 6-inch nominal intervals to a depth of 18 inches below the subgrade surface. Sensor cables were buried within the subgrade.

The sensors, which are manufactured by Bison Instruments, Inc., Minneapolis, Minn., are individual disk-shaped coils that operate through electromagnetic mutual inductance coupling of any two sensors. The sensors are not interconnected and are "free floating" in the soil, thereby contributing minimal interference to soil movement. The disks were connected by coaxial cable to a Bison Instruments' model 4101A soil strain instrument which contained the driving, amplification, balancing, calibration, and recording controls. Spacing resolution with this system was 0.0001 inch, and laboratory bench tests indicated that spacing measurement was repeatable to within +0.0032 or -0.0030 inch.

PAVEMENT CONSTRUCTION

After installation of the soil strain sensors, a layer of 6-mil-thick polyethylene was placed over the clay subgrade to function as a moisture barrier between the foam and clay. A single layer of 4020-weight* fiberglass mat was placed over the polyethylene. The fiberglass layer was comprised of four strips of 78 inches wide fiberglass mat with a 12-inch lap between strips. Three construction joints were fabricated and were oriented with the traffic direction at 5, 10, and 15 feet from the test pit edge (Figure 4).

The construction joints were fiberglass angle shapes having aluminum honeycomb bonded to the vertical legs and 4020-weight fiberglass mat

*40 oz/yd^2 of woven roving plus 2 oz/ft^2 of chemically bonded, chopped strand fiberglass.

Table 1. Subgrade Density and Moisture Content Test Data[a]

Location	Depth (in.)	Wet Density (pcf)	Dry Density (pcf)	Moisture Content (%)
1	2	123.1	95.7	28.6
	6	120.3	92.1	30.7
	12	123.9	96.0	29.1
2	2	125.7	98.7	27.4
	6	125.6	98.3	27.7
	12	126.3	99.0	27.6
3	2	123.5	95.9	28.7
	6	125.4	97.5	28.6
	12	125.7	98.4	27.7
4	2	121.9	92.3	32.1
	6	121.3	91.4	32.7
	12	123.4	93.5	31.9
5	2	122.8	94.2	30.4
	6	123.3	93.9	31.3
	12	125.1	96.7	29.4
6	2	122.1	93.7	30.3
	6	123.0	94.1	30.7
	12	124.5	96.4	29.1
7	2	122.1	93.9	30.0
	6	122.5	94.1	30.2
	12	124.9	95.7	30.5
8	2	124.1	94.9	30.8
	6	125.0	96.8	29.1
	12	126.7	97.7	29.6
9	2	121.9	93.2	30.9
	6	123.4	95.2	29.5
	12	125.8	97.3	29.2

[a]Tests conducted in accordance with ASTM Test Designation: D2922-71 (Ref 4).

bonded to the horizontal legs (Figures 5 and 6). The 5 x 5-inch FRP angles are commercially available and are manufactured by the pultrusion* process. Mechanical properties of the angles are given in Table 2. During application of the foam, the joints function as forms on either side of the paving lanes to contain the initially fluid polyurethane resin until rise and set are completed. After cure of the foam, the joints structurally bond adjacent lanes of the finished pavement - the fiberglass matting transfers tension and the honeycomb transfers shear.

Polyurethane foam was spray-applied (Figure 7) after placement of the construction joints. The foam, CPR 739 at 20 pcf density, was spray-applied one paving lane at a time. Spraying was accomplished with bench model apparatus (Appendix B) specially manufactured for the project by Johnson and Sons, Glendale, Calif. The two-component foam was mixed by each component passing through baffles of a static mixing element in the barrel of the spray gun and was discharged (sprayed) at a rate of approximately 30 lb/min. Approximately 40 minutes were required to spray the foam for a paving lane. Continuous strand glass fiber, style 535, from PPG Industries was fed into a chopper device attached to the spray gun and was cut into strands 1 inch long. The gun then blew the fibers into the foam spray pattern, thereby mixing the foam and fibers. The polyurethane resin was sprayed onto the fiberglass mat, partially penetrating the mat; and, after rising and curing, the glass-fiber-reinforced foam was completely bonded to the mat.

Several difficulties were encountered during the spray application of foam:

1. Inability to gage accurately the quantity of deposited resin to control finish core thickness
2. Improper spray pattern, resulting in poor foam and glass fiber mixing
3. Insufficient glass mixed into the foam
4. Low foam density
5. Splitting of the foam core
6. Uneven foam rise

These problem areas are discussed in more detail later in this document. Problem areas 1 and 6 coupled to produce low spots in the foam surface, even after trimming (Figure 8), which later contributed to localized bond deficiencies between the foam core and FRP facing.

The inherent uneven rise of the foam coupled with the inability of the spray gun operator to evenly distribute the foam made trimming of the cured foam a necessity. The foam surface was trimmed using a model CP-V concrete planer** made by Equipment Development Company (EDCO),

*A method combining extrusion and pulling of the material in the manufacturing process.

**The planer represents commercially available equipment which was adaptable for the limited quantity of trimming required for the test section. It is not representative of conceptual equipment for trimming large field sections (refer to Ref 1).

Table 2. Mechanical Properties of Extren Series 525 Fiberglass Angles (Ref 5)

Property	Value
Mechanical (coupon)	
Longitudinal Direction	
Ultimate Tensile Strength, psi	30,000
Ultimate Compressive Strength, psi	20,000
Ultimate Flexural Strength, psi	30,000
Tensile Modulus, psi x 10^6	2.3
Compressive Modulus, psi x 10^6	2.3
Flexural Modulus, psi x 10^6	1.3
Ultimate Shear Strength, psi	4,500
Ultimate Bearing Stress, psi	20,000
Izod Impact Strength (ASTM-D256), ft-lb/in. of notch (Sample Thickness - 1/8 in.)	18
Transverse Direction	
Ultimate Tensile Strength, psi	5,000
Ultimate Compressive Strength, psi	10,000
Ultimate Flexural Strength, psi	10,000
Tensile Modulus, psi x 10^6	0.8
Compressive Modulus, psi x 10^6	1.0
Flexural Modulus, psi x 10^6	0.6
Ultimate Shear Strength, psi	4,500
Ultimate Bearing Stress, psi	20,000
Izod Impact Strength (ASTM-D256), ft-lb/in. of notch	4
Barcol Hardness	50
Mechanical (full section in bending)	
Modulus of Elasticity, psi x 10^6	2.3
Tensile Strength, psi	20,000
Compressive Strength, psi	20,000
Electrical	
Electric Strength, short term in oil 1/8 in. (ASTM-D149), vpm	200
Electric Strength, short term in oil, kV/in.	25
Dielectric Constant, 60 Hz, (ASTM-D150)	5.0
Dissipation Factor, 60 Hz, (ASTM-D150)	0.03
Arc Resistance (ASTM-D495), sec	80

(Continued)

Table 2. (Continued)

Property	Value
Thermal	
Thermal Coefficient of Expansion (ASTM-D696), in./in./°F	5×10^{-6}
Thermal Conductivity, Btu/ $ft^2/hr/°F/in.$	4
Specific Heat, Btu/lb/°F	0.28
Miscellaneous	
Density (ASTM-D792), lb/in^3	
Solid Shapes	0.062
Hollow Shapes	0.064
Specific Gravity (ASTM-D792)	
Solid Shapes	1.72
Hollow Shapes	1.78
Water Absorption (24 hour immersion) (ASTM-D570), max. % by weight	0.75

Frederick, Md. The EDCO planer has a series of carbide steel-toothed (cogged) rings mounted on four cutting bars (Figure 9), and it provides a 5-inch-wide cutting path. A completely plane surface was difficult to produce with the concrete planer because it did not have a true surface to ride upon. The planer did produce, however, a rough texture which was conducive to a high quality bond between the foam core and the FRP facing.

During trimming, numerous voids (i.e., horizontal cracks were detected in the interior of the foam (refer to CONSTRUCTION PROBLEMS). Two voids were repaired by removing the foam down to the void, placing foam within the resultant hole, and temporarily capping the hole during the rising process, thus forcing the expanding foam into all recesses of the void. The technique was time-consuming and not entirely satisfactory structurally. A rapid void repair technique was developed which consisted of drilling several 1/2-inch-diam holes in the foam to the void and forcing liquid foam resin into the void with the spray gun (without spray nozzle) until foam was observed exiting from adjacent holes. Reaction of the components and the accompanying expansion and pressure forced the foam into all recesses of the void and a structurally adequate repair was completed in a matter of minutes. This nondestructive repair technique could easily be applied in the field to repair the foam core of the FIBERMAT if it became damaged by traffic or enemy action.

After trimming, two layers of 4020-weight fiberglass mat were placed over the foam. Each layer was comprised of several strips of fiberglass (6-1/2-foot width) which were lapped by 12 inches. Polyester resin (PPG Industries RS 50338) was mixed manually with catalyst and promoter in 40-liter batches. The catalyzed resin was then poured onto the fiberglass mat and spread with aluminum rollers. After the resin penetrated and saturated the fiberglass, the laminate was rolled to expel trapped air. The resin was mixed with too much catalyst and promoter. Consequently, gel time was approximately 10 minutes instead of an anticipated time of 30 minutes. This was insufficient time to complete saturation of the fiberglass in several localized areas (particularly at laps where there were three layers of fiberglass instead of the typical two). The fast resin cure also contributed to localized crazing* of the resin and shrinkage of the laminate. Three factors - low spots in the foam substrate, incomplete saturation of the fiberglass, and excessive shrinkage - combined to produce numerous localized defects within the completed FIBERMAT pavement where the FRP facing was not bonded to the foam substrate.

The FIBERMAT pavement was instrumented in several locations (Figure 3) to record strain produced in the pavement by the static wheel load. Ailtech model CG-129 strain gages (distributed by Cutler-Hammer Company, Industry, Calif.) were implanted in the bottom of the foam core. A typical gage consisted of a self-temperature-compensated, nickel-chrome, strain-sensing filament encased within a twisted stainless steel tube. The CG-129 gage has a rated strain level of ±20,000 μin./in. with an apparent strain at temperature of ±50 μin./in. (Ref 6). The 2-inch-long gages were obtained from the manufacturer without the locating disks, which are normally provided as an integral attachment at both ends of the gage. The gages were inserted within the weave of the fiberglass

*Cracking of pooled resin at the fiberglass surface did not appear to affect the strength.

mat, which was used as foam reinforcement. After foam spraying, the gages were firmly bonded within approximately 1/2 inch of the bottom of the foam core.

Model EA-41-250BG-20 strain gages (0.25-inch gage length), produced by Micro-Measurements, Romulus, Mich., were affixed to the surface of the FRP facing of the completed FIBERMAT pavement. The FRP surface was prepared by light sanding with a no. 300 grit sandpaper followed by cleaning with isopropyl alcohol. The gages were bonded with M-Bond type AE epoxy.

CONSTRUCTION PROBLEMS AND POSSIBLE SOLUTIONS

The 20-ft^2 FIBERMAT pavement constructed for the traffic test is the current largest field-fabricated section of FIBERMAT. The section was built with experimental bench-model equipment. Construction of the test section, therefore, afforded an opportunity to observe some of the problems and to discover solutions which could be of benefit to later research efforts directed to prototype equipment development and formulation of field construction techniques.

1. Finish Core Thickness: Finish core thickness is impossible to predict when using manual spray application. This problem may be correctable in prototype equipment through reliance on sensors instead of human judgment to control deposit rate.

2. Spray Pattern: For the first two paving lanes, the polyurethane resins were at too low a temperature; this produced too high a viscosity for a proper spray pattern to be developed. Mixing of fiberglass and foam was adversely affected by the poor pattern. A correct pattern was obtained when the resins were warmed to approximately 90°F before spraying.

3. Low Fiberglass Content: Fiberglass content was approximately 2% by weight instead of the required 10%. The low content was caused by the resin not properly "wetting out" the chopped glass fibers. Fiber-to-resin compatibility may be improved through use of a different type of continuous strand; e.g., PPG Industries style 526 does not fray as readily during high speed chopping and would exhibit improved lay-down and wet-out characteristics.

4. Low Density: Laboratory tests of field samples indicate a foam density of 17 pcf instead of the design density of 20 pcf. The reduction was caused by the high velocity passage of mixed foam resin through the orifice of the spray gun nozzle. Density, when using a spray system, could be corrected by either redesign of the nozzle or switching to a foam with a higher nominal density; e.g., 25 pcf, which would give the requisite 20-pcf field density.

5. Core Splitting: Large horizontal voids within the foam core were a result of incompatibility of the foam resin and continuous strand fiberglass and/or excessive exotherm created by the curing of the 5-inch-thick core. Splitting of the core could be reduced by altering the fiberglass type as previously recommended, by constructing a thinner core, or by building the core in two or more passes.

6. Uneven Rise: The foam rises with undulations of approximately ±1/2 inch. This unevenness may be partially rectified by automatic, sensor-directed, dispensing equipment; however, either trimming of the foam and/or a type of forming system will remain a requirement.

TRAFFIC TESTING

Traffic Definition

The FIBERMAT was trafficked with a load cart (Figure 10) which was specially designed to simulate a main gear of a fully loaded F-4 Phantom aircraft. The load cart is equipped with an outrigger wheel to prevent overturning and is powered by a front-wheel-drive truck. Lead weights are centered over a 30-7.7, 18-ply rated tire inflated to 267 psi. With a 27,000-pound wheel load, the tire had a contact area of about 102 $in.^2$.

Traffic was applied to simulate the traffic distribution pattern that would be encountered in actual aircraft takeoffs and landings. The pattern approaches a statistically normal distribution curve (Ref 7). Traffic was started on one side of the traffic lane, and the load cart was driven forward and backward in the same path for the length of the traffic lane. The path of the cart was shifted laterally 10 inches (width of the tire print) on each successive forward trip. The interior 100 inches of the traffic lane was trafficked for six additional coverages. The center 60 inches of the traffic lane received two additional coverages for a total of 10 coverages. The net result was that the center 60-inch-wide strip of the traffic lane received 100% of the traffic, the 20-inch-wide strips on either side of the center 60 inches received 80%, and the single 10-inch-wide outside strips received only 20% (Figure 11). A total of 96 passes of the load cart were required to complete 10 coverages of the center of the traffic lane.

Traffic Section Performance Data

Data were recorded for the FIBERMAT test section at intervals of 0, 50, 100, 150, 200, 250 and 300 coverages. Recorded data included:

1. Elastic deflection beneath the static test wheel
2. Permanent pavement deformation, including longitudinal and cross section profiles
3. Soil strain beneath the test wheel
4. Pavement strain

Immediately before trafficking, the load cart was driven onto the test section and the wheel was successively parked over each of the three data recording stations (Figure 3). Strain data for the FRP were obtained only during the initial recording at 0 coverages, since the gages were surface mounted and susceptible to damage by trafficking. The strain gages imbedded within the foam at location PS2 were damaged during construction, and the soil strain gages at location SS1 functioned improperly - a short developed and after 100 coverages the gages were inoperable. All other instrumentation was in proper order.

Performance data were recorded for the test section to enable correlation with an analytical prediction of the system behavior which was derived using the finite element technique and a computer program, SLIP (Ref 8). Triaxial tests were conducted on samples of Wewahitchka clay used by the AFESC as subgrade material, and its elastic modulus at the predicted stress level was determined using the secant method. Test section material properties were provided as input to the program, which generated output of stress, strain, and deformation quantities for the idealized FIBERMAT pavement system (Appendix C).

The measured elastic deflection of the FIBERMAT at 0 coverages was 1/8 inch (Table 3). The deflection was recorded using a 4-foot straightedge positioned alongside the tire at approximately 8 inches from the tire centerline (Figure 12). This measured deflection point correlated well with the computer-predicted deflection profile (Figure 13). The vertical soil strain beneath the wheel load centerline was also recorded and found to agree closely with the predicted strain (Figure 14). A slight decrease in measured strain was observed with increasing coverages which may be indicative of stiffening of the clay subgrade. Close agreement was also observed for strain within the FIBERMAT pavement (Figure 15).

Table 3. Maximum Recorded Deflections

Coverages	Deflections (in.) at Following Locations--		
	D1	D2	D3
0	1/8	1/16	1/4
50	1/8	0	1/2
100	3/4	0	1/2
250	--	1/2	1/2

Trafficking

After construction of the FIBERMAT pavement, there was a section within paving lane no. 3 approximately 2 x 2 feet where the foam core and FRP facing were not bonded.* Although the deficiency could have been repaired by pumping polyester resin between the FRP facing and foam core, no equipment was available. Therefore, traffic was initiated. The section was found to be very trafficable with only a 1/4-inch elastic deflection recorded beneath the wheel load. The unbonded area within paving lane no. 3 gradually increased in size and had reached 3 x 6 feet in dimension when the lane failed at 136 traffic coverages. Failure consisted of a longitudinal tear, 3 feet in length, in the FRP facing over the unbonded area. An elastic deflection of 5/8 inch had been recorded beneath the wheel load for the failure location at 120 coverages.

*A result of uneven foam surface and rapid polyester resin gelation.

Trafficking was resumed for only the southern half of the traffic lane with the same traffic distribution originally utilized for that portion. At 190 coverages, an area 4 x 5 feet in plan dimension within paving lane no. 2 had delaminated,* although it was adequately supporting traffic. Two layers of FRP (1/4-inch finish thickness) were laminated to the original FRP facing to produce a surface patch measuring 6 x 6.5 feet. The patch performed well (7/8-inch elastic deflection after 300 coverages, Figure 16), and traffic was continued to 310 coverages at which point the entire test section was considered failed. Instability of the load cart when transitioning from the portland cement concrete (PCC) pavement of the test facility to the test section was the determining failure criterion. After trafficking, the FIBERMAT was further tested, without any indication of damage, by rolling the test wheel over an aircraft arresting cable 20 times in one location (Figure 17).

The concrete along the eastern and western edges of the test section was severely spalled from previous traffic tests conducted by the AFESC. After constructing the FIBERMAT pavement, the spalled edges were temporarily repaired using polyurethane foam. This spall repair did not adequately support the load cart tire, and the repair had to be repeated several times during the trafficking. The trafficked edges of the FIBERMAT pavement therefore received an inordinate amount of static and impact loading during the transitioning of the load cart onto and from the test section. Deflection was more pronounced along the FIBERMAT edges than would have been the case with better load transfer. Eventually, trafficking was terminated because of excessive FIBERMAT deflection (>1 inch) at the edges during transition of the load cart to and from the PCC pavement.

Stations were marked at 1-foot intervals along three lines (Figure 18) on the FIBERMAT and elevations were recorded at intervals during the trafficking to enable plotting of the profile of the pavement surface (Figures 19 and 20). Overall the pavement exhibited elastic behavior with essentially no permanent deformation. Permanent deformation of approximately 1 inch was recorded for line C-C at 12 feet from the northern edge, which was the location of the FRP facing failure in paving lane no. 3 at 136 traffic coverages.

TRAFFICABILITY SUMMARY

FIBERMAT expedient pavement was tested for endurance to simulated medium-duty (F-4) aircraft traffic. The pavement section consisted of a fiberglass-reinforced, 5-inch-thick core of 20-pcf-density rigid polyurethane foam bonded to an upper facing of 1/4-inch-thick fiberglass-reinforced polyester resin (FRP). The traffic was applied with a load cart having a 30-7.7, 18-ply-rated tire loaded to 27,000 pounds and inflated to a pressure of 267 psi. The traffic was applied in a distributed pattern.

*This large delamination had gradually increased in dimension during trafficking from a smaller unbonded section measuring approximately 2 x 2 feet, which was produced during pavement construction.

Problems encountered during construction of the pavement produced localized areas with deficient structural integrity in the core-to-facing bond. These defects were enlarged by trafficking and eventually caused pavement failure. The pavement performance was satisfactory to 136 coverages (1,306 passes) of the load cart when a tear developed in a section of the third paving lane. Neither repair nor replacement of the damaged area was attempted after the failure. Traffic was continued with the same pattern on the remaining half of the traffic lane for 174 additional coverages. Traffic was discontinued at 310 coverages (2,141 passes) as a result of load cart instability when transitioning from the test section to the concrete pavement of the test facility.

The FIBERMAT pavement exhibited good endurance and toughness. Although locally failed according to structural criteria in several locations before initiation of traffic, the pavement sustained the applied traffic with only slight elastic deflection. The top facing of FRP and the lower fiberglass mat reinforcement were continuous throughout the pavement and efficiently carried the moving wheel load across localized failures of core-to-facing bond. Elastic deflection recorded beneath the test wheel was on the order of 1/4 inch which compares favorably with the elastic deflection of 3/4 inch recorded for AM2 matting during similar previous traffic tests (Ref 9).

CONCEPT FEASIBILITY

Traffic Life

FIBERMAT constructed over a soil having a CBR of 5.9 withstood 310 coverages of a 27,000-pound wheel load at 267 psi tire pressure. Currently, AM2 airfield matting is stockpiled by the Marine Corps for expedient surfacing of expeditionary airfields (EAF). FIBERMAT would augment or replace AM2 matting. Therefore, the traffic performance of AM2 represents a baseline for feasibility determination.

Table 4 lists the performance parameters for AM2, which was traffic-tested by the Army Corps of Engineers at the Waterways Experiment Station (WES), Vicksburg, Miss. (Ref 9 and 10) during engineering development by the Naval Air Engineering Center. The FIBERMAT and AM2 traffic tests were conducted with several variables present - tire pressure, wheel load, and soil strength. Thus, a method is required which would enable a valid comparison. Studies conducted by WES (Ref 11) during development of the CBR design method for flexible pavements have indicated a logarithmic relationship between flexible pavement thickness, soil strength, wheel load, tire pressure, and traffic as follows:

$$\frac{t}{0.23 \log_{10}(C) + 0.15} = \sqrt{P\left(\frac{1}{8.1\ CBR} - \frac{1}{p\pi}\right)}$$

where t = design thickness of flexible pavement structure, in.

C = coverages at failure

P = total wheel load, lb

CBR = rated California Bearing Ratio of subgrade

p = tire pressure, psi

Although this empirical relationship was developed for the design of conventional flexible pavements, it has been used by WES (Ref 12) to extrapolate the performance of expedient airfield mattings. The performance variables from a traffic test – soil strength, tire pressure, wheel load, and traffic coverages – are entered into the equation, and the equation is solved to determine the thickness, t. The thickness thus solved is for an equivalent built-up thickness, t, of a conventional flexible pavement system and is not the thickness of the matting. Thus, the load distribution of an airfield matting system has been considered analogous to that of a given thickness of flexible pavement. In the WES reports of matting traffic tests, the equation is first solved for t; and then when this value of t and a different CBR value are used, the equation is re-solved to extrapolate a given matting's performance (traffic life) for a different soil strength than that represented by the traffic test conditions.

For the current study the relationship was found useful for the correlation of the traffic performance of the two dissimilar expedient surfacings – FIBERMAT and AM2 matting. By entering the various performance variables recorded during traffic tests for each surfacing and solving the equation for t, a comparison was made of the relative performance of the dissimilar surfacings by relating surfacing performance to an equivalent thickness of flexible pavement. The equation, as originally developed, represents the required pavement thickness to prevent excessive deflection of underlying layers in a built-up pavement system resulting from repetitions of load. Thus, the more competent expedient surfacing would be represented by a larger value of t – its performance would equate to that of a thicker built-up pavement system. Solutions of the equation produced the following results:

Surfacing	Equivalent Built-up Pavement Thickness, t (in.)
FIBERMAT	16.7
AM2 (Harvey Election Beam Welded, Apr 1969)	20.9
AM2 (Harvey, Sep 1969)	20.6

FIBERMAT was thus found to be a less capable surfacing than AM2 matting; however, several relevant factors should be evaluated.

Table 4. Performance Parameters of AM2 Airfield Matting

Harvey AM2 Matting Type	Traffic Test Date and Reference	Wheel Load (lb)	Tire Pressure (psi)	Average Subgrade CBR (%)	Coverages at Failure
Electron Beam Welded, MOD 2	Apr 1969 (Ref 10)	27,000	400	4	346
Production	Sep 1969 (Ref 9)	27,000	400	3.8	258

For the AM2 traffic tests, up to 10% of the mat planks were permitted to be replaced, and failure of the test section was preceded by failure of an additional 10% of the planks (a total of 20% failed). In contrast, none of the pavement within the FIBERMAT test section was replaced, although a patch representing 1.5% of the test section material was utilized. Furthermore, several defects which were built into the pavement structure precipitated a premature failure. An improvement in construction techniques would have a significant effect on pavement trafficability. The primary failure mode was debonding between the core and upper facing produced through intensification of construction defects. These defects would be eliminated by the introduction of prototype fabrication equipment. Furthermore, these defects and any traffic-induced debonding could be repaired rapidly, at low cost, with commercially available equipment for low volume pumping of polyester resin. Such equipment would have the potential for producing a large improvement in traffic life.

The FIBERMAT test section did not exhibit traffic life equivalent to that of AM2. FIBERMAT did demonstrate excellent potential, however, for a substantial trafficability improvement over AM2. Given the above mitigating factors, the FIBERMAT concept is considered feasible with respect to trafficability. Additional traffic testing is warranted after improvement of field construction and repair techniques.

Logistics

FIBERMAT was traffic-tested on a low strength clay subgrade to demonstrate that the pavement could be designed to provide adequate trafficability for such a soil and to facilitate comparisons with AM2 airfield matting, which has been extensively traffic-tested on clay soil having CBR values of approximately 4. Although this FIBERMAT traffic test has shown that FIBERMAT is capable of emplacement on a soil of CBR 4, for logistic economy it is recommended that the lowest strength soil for FIBERMAT usage be set at a higher CBR value.

The design of AM2 matting for service over a weak soil is valid since an AM2-surfaced airfield consists of thousands of joints. Even if AM2 were to be placed over a compacted subgrade of high CBR rating and, if any cohesive material were present, infiltration of rain water through the joints and subsequent aircraft traffic would cause a substantial loss of subgrade support. The FIBERMAT concept, however, entails construction of a continuous pavement with very few water-tight expansion and contraction joints (approximately 200 feet on center). Thus, if FIBERMAT were constructed on a compacted subgrade with adequate grading provided for drainage, the subgrade would retain the majority of its strength even when containing cohesive materials. The construction of an EAF requires cutting and filling operations to build a runway having grade changes suitable for aircraft operation and allowing for proper drainage. As an estimate, the earthwork involved, with only incidental compaction, should result in a minimum soil CBR value on the order of 10; thus, a CBR of 10 is recommended as the minimum soil strength for FIBERMAT pavement section design. FIBERMAT pavement section depths may be reduced for instances of documented higher soil strength or reduced wheel and tire pressure loadings.

An analysis (Appendix D) was undertaken whereby EAF traffic areas were defined and FIBERMAT pavement sections were designed for these traffic areas with the F-4B as the critical aircraft. The logistic

factors for the airfield were summarized (Table D-4) and were used to construct descriptive parameters which would facilitate comparison with an AM2 matting baseline to give an indication of relative logistic performance and benefit (Table 5). Because AM2 matting is prefabricated, it exhibits constant logistic factors independent of soil strength. FIBERMAT, in contrast, would become logistically more advantageous with increasing soil strength. When constructed on soil having a CBR of 10, the estimated savings in cost for the FIBERMAT-surfaced airfield (considering all traffic areas) would be approximately 68%. Concurrently, shipping cube requirements would be reduced by 59%, based upon a containerized mode of shipment (20% for breakbulk). Weight requirements would be reduced by 26%.

Table 5. Relative Logistic Performance of AM2 Matting and FIBERMAT for a Containerized Shipping Mode[a]

Type of Mat	Cost ($/ft)	Cube Ratio[b] (ft^2/ft^3)	Weight (psf)
FIBERMAT (All Traffic Areas) (CBR10)	3.89	6.5	4.8
FIBERMAT (Areas C, C1 and D) (CBR10)	6.43	4.2	7.4
AM2 (CBR4)	12.00[c]	2.7[d]	6.5

[a]FIBERMAT estimates based upon surfacing the traffic areas of the EAF depicted in Figure D-1.

[b]Ft^2 of ground coverage per ft^3 of shipped material.

[c]The 1980 cost for AM2 MOD4 electron beam welded matting was established in a telephone conversation with Ms. D Braun, AM2 Product Manager, Martin Marietta Corp., Los Angeles, Calif.

[d]Using Reference 13, cube ratio is calculated at 5.2 ft^2/ft^3 for a breakbulk shipping mode.

The foregoing projection was based upon average logistic parameters for the construction of all traffic areas. A large percentage of the benefits was derived from the extensive use of FRP in the parking apron. When considering only FIBERMAT-surfaced traffic areas - areas C, C1 and D - the estimated cost saving is 46%. Shipping cube requirements would be reduced (related to AM2) by 36% for a containerized mode (increased by 24% for breakbulk). Weight requirements are increased (relative to AM2) by 14%.

Thus, the FIBERMAT concept offers benefits for all logistic parameters (with the exception of a slight weight penalty for designs at soil CBR of 10) for containerized shipment. These benefits decline when considering a breakbulk mode of shipment, although the critical parameters - cube and weight - approach the breakeven point. A soil strength of CBR 10 is a minimum value, and FIBERMAT logistic parameters would improve with increasing soil strength. In conclusion, the FIBERMAT concept remains feasible with regard to logistic benefit when constructed on a soil having a minimum CBR value of 10.

CONCLUSIONS AND RECOMMENDATIONS

The traffic test conducted at the Rapid Runway Repair (RRR) Test Facility of the AFESC has demonstrated the endurance of FIBERMAT to repeated simulated F-4 aircraft traffic when placed over a soil having a CBR value of 5.9. Although not surpassing the performance of AM2 matting, the pavement sustained a maximum of 310 traffic coverages (2,141 passes) and has potential for increased life in excess of that of AM2 upon development of improved construction techniques. The concept is considered feasible with respect to traffic life.

Data obtained during the trafficking have validated the accuracy of analyses of FIBERMAT sections using the finite element computer code SLIP. This code was used to design additional pavement sections for a soil having a CBR value of 10 to enable a determination of logistic feasibility. The FIBERMAT concept is concluded to remain logistically feasible for emplacement of the pavement on soils having minimum CBR values of 10.

The following recommendations are presented:

1. Continue project development with the formulation of concepts for field construction, including fabrication techniques and equipment.

2. Develop a forming method for restraining the foam during rise, thereby significantly reducing trimming requirements and lowering material costs.

3. Investigate alternative styles of fiberglass roving for compatibility with the foam components and chopper operation.

4. Investigate the use of a higher density CPR-739 foam to offset the reduction in foam density which accompanies high velocity passage through a spray nozzle.

5. Conduct another traffic test (F-4 load cart, soil CBR of 10) upon refinement of construction technique.

ACKNOWLEDGMENTS

The valuable assistance and dedication of Mr. Leonard Woloszynski and Mr. Larry Underbakke, civil engineering technicians at CEL, in the construction of the FIBERMAT pavement and installation of instrumentation are gratefully acknowledged. Appreciation is also expressed to the Air

Force Engineering and Services Center for the use of the Rapid Runway Repair Test Facility, preparation and testing of the clay subgrade, and surveying and trafficking of the test section.

REFERENCES

1. Civil Engineering Laboratory. Technical Note N-1553: Multipurpose expedient paving system (MEPS) for expeditionary airfields - an interim report, by P. S. Springston. Port Hueneme, Calif., Apr 1979.

2. _____. Technical Note N-1472: Expedient structural sandwich soil surfacing of fiberglass reinforced polyester and polyurethane foam, by M. C. Hironaka, R. B. Brownie, and S. Tucillo. Port Hueneme, Calif., Feb 1977.

3. Department of Defense. Military Standard No. MIL-STD-619: Unified soil classification system for roads, airfields, embankments and foundations. Washington, D.C., Jun 1968.

4. "Test Designation D2922-71: Determining the density of soil and soil aggregate in place by nuclear methods (shallow depth)," 1972 Annual Book of ASTM Standards, Part II, American Society for Testing and Materials, Philadelphia, Pa., Apr 1972.

5. Morrison Molded Fiberglass Company. Form MMFG 877-3: MMFG EXTREN® fiberglass reinforced pultrusions for construction, Bristol, Va.

6. Ailtech. Embedment gage, model CG129, specifications. Cutler-Hammer Company, Industry, Calif.

7. Army Engineer Waterways Experiment Station, Civil Engineering. Miscellaneous Paper No. 5-73-56: Lateral distribution of aircraft traffic, by D. M. Brown and O. O. Thompson. Vicksburg, Miss., Jul 1973.

8. Naval Civil Engineering Laboratory. Technical Report R-763: Layered pavement systems - Part I. Layered system design; Part II. Fatigue of plain concrete, by J. B. Forrest, M. G. Katona, and D. F. Griffin. Port Hueneme, Calif., Apr 1972.

9. Army Engineer Waterways Experiment Station, Civil Engineering. Miscellaneous Paper No. S-69-41: Evaluation of Harvey and Kaiser production AM2 landing mat, by C. D. Burns and R. W. Grau. Vicksburg, Miss., Sep 1969.

10. _____. Miscellaneous Paper No. S-69-13: Evaluation of Harvey electron beam welded AM2 landing mat (AM2 MOD 2), by C. D. Burns and D. P. Wolf. Vicksburg, Miss., Apr 1969.

11. _____. Instruction Report No. 4: Developing a set of CBR design curves, by R. G. Ahlvin. Vicksburg, Miss., Nov 1959.

12. _____. Miscellaneous Paper No. S-72-40: Evaluation of Dow Chemical extruded truss-web landing mat, by D. W. White, Jr. Vicksburg, Miss., Dec 1972.

13. Naval Air Systems Command. NAVAIR 51-35-7: Expeditionary airfields; logistics data to field installation. Philadelphia, Pa., Mar 1974.

14. Civil and Environmental Engineering Development Office. Technical Report TR 79-14: Field test of expedient pavement repair. Tyndall AFB, Fla. (In Publication)

15. Air Force Civil Engineering Center. Technical Report TR-75-24: Bomb damage repair and damage prediction, by George W. Brooks, John E. Cunningham, and Paul W. Mayer. Tyndall AFB, Fla., Oct 1975.

16. Civil and Environmental Engineering Development Office. Technical Report TR-78-44: Laboratory evaluation of expedient pavement repair materials, by R. Rollings. Tyndall AFB, Fla., Jun 1978.

17. D. E. Daniel and R. E. Olson. "Stress-strain properties of compacted clays," Journal of the Geotechnical Engineering Division, American Society of Civil Engineers, vol. 100, no. GT10, Oct 1974.

18. Civil Engineering Laboratory. Technical Note N-1563: Fiberglass reinforced plastic surfacing for rapid runway repair by Naval construction forces, by P. S. Springston. Port Hueneme, Calif., Oct 1979.

19. Federal Aviation Administration. Report No. FAA-RD-76-206: Experimental relationships between moduli for soil layers beneath concrete pavements, by J. B. Forrest, P. S. Springston, M. G. Katona, and J. Rollins. Washington, D.C., Jun 1977.

20. Civil Engineering Laboratory. Technical Note N-1572: Traffic testing of a fiberglass-reinforced polyester resin surfacing for rapid runway repair, by P. S. Springston. Port Hueneme, Calif.

21. Telephone conversation between Maj. Richardson, USMC, Marine Corps Development and Education Command, and P. S. Springston, Civil Engineering Laboratory, Dec 1979.

22. Air Force Weapons Laboratory. Technical Report AFWL-TR-69-54: Aircraft characteristics for airfield pavement design and evaluation, by D. R. Hay. Kirtland AFB, N.Mex., Oct 1969.

23. Naval Air Systems Command. NAVAIR 01-245FDD-1: NATOPS flight manual, Navy Model F-4J aircraft. Philadelphia, Pa., Jun 1969.

Abbreviations and Nomenclature

Abbreviations

AFESC	Air Force Engineering and Services Center
AOA	Amphibious objective area
CAS	Calibrated airspeed
CBR	California Bearing Ratio
CH	Heavy clay as defined in Uniform Soil Classification System
EAF	Expeditionary airfield
ESWL	Equivalent single wheel load
FRP	Fiberglass-reinforced polyester resin
MEPS	Multipurpose expedient paving system
PCC	Portland cement concrete
RRR	Rapid runway repair
WES	Waterways Experiment Station (Army)

Nomenclature

C	Coverages at failure
D	Deflection measurement point
E	Young's elastic modulus, psi
E_b	Young's modulus (in bending), psi
E_c	Young's modulus (in compression), psi
E_s	Young's modulus for soil, psi
LL	Liquid limit
p	Tire pressure, psi
P	Total wheel load, lb
PI	Plasticity index
PL	Plastic limit
PS	Pavement strain measurement point
r	Load radius, in.
R	Mesh radius, in.
SS	Soil strain measurement point
t	Design thickness of flexible pavement structure, in.

(continued)

Nomenclature (continued)

z	Depth below load surface, in.
γ_d	Soil dry density, pcf
ν	Poisson's ratio
σ_b	Normal stress (in bending), psi
σ_c	Normal compressive stress, psi
σ_{max}	Maximum principal normal stress, psi
σ_{min}	Minor principal normal stress, psi
σ_r	Radial normal stress, psi
σ_z	Vertical normal stress, psi
σ_1	Axial stress, psi (triaxial compression test)
σ_3	Confining stress, psi (triaxial compression test)
ε_z	Vertical (axial) strain, μin./in.
τ_{max}	Maximum principal shear stress, psi
τ_{ULT}	Ultimate shear stress, psi
ω	Soil moisture content (percent by dry weight)

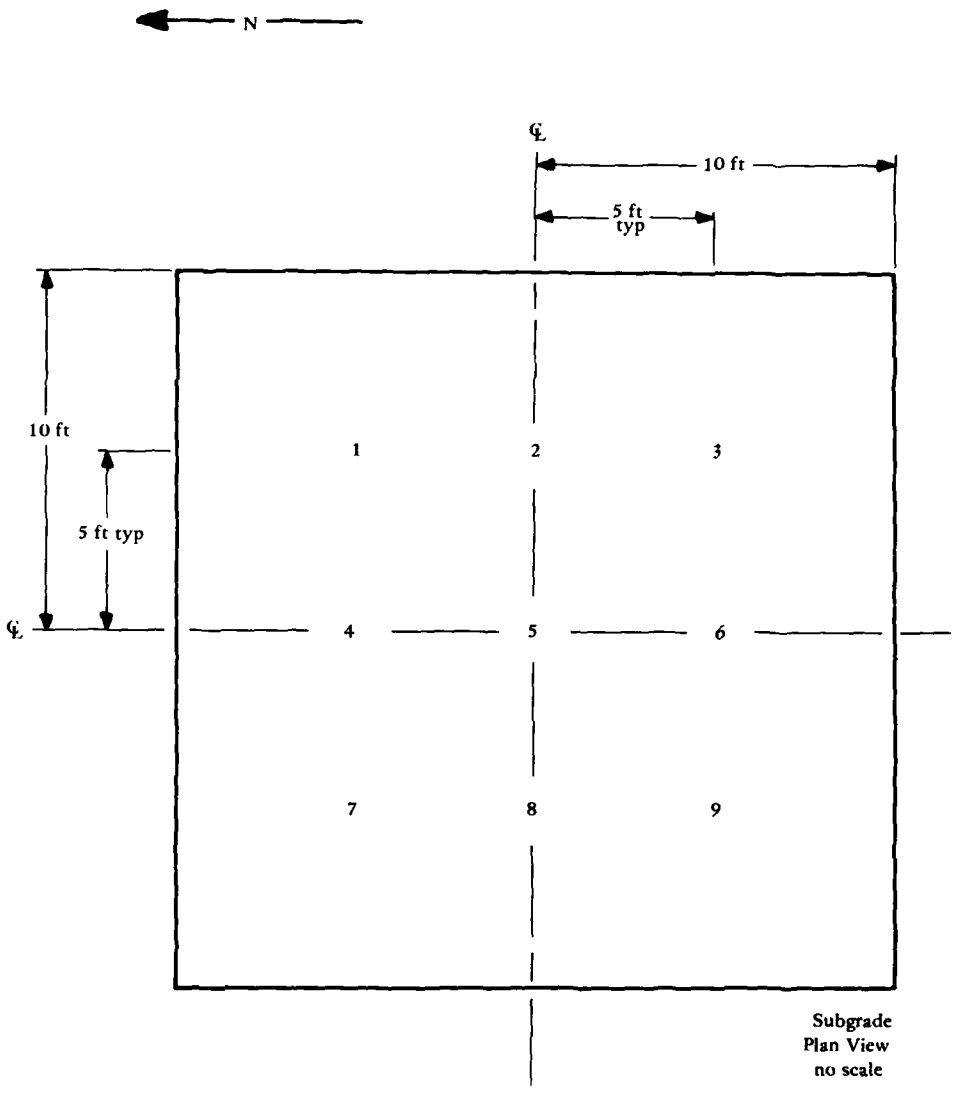

Figure 1. Moisture-density test locations.

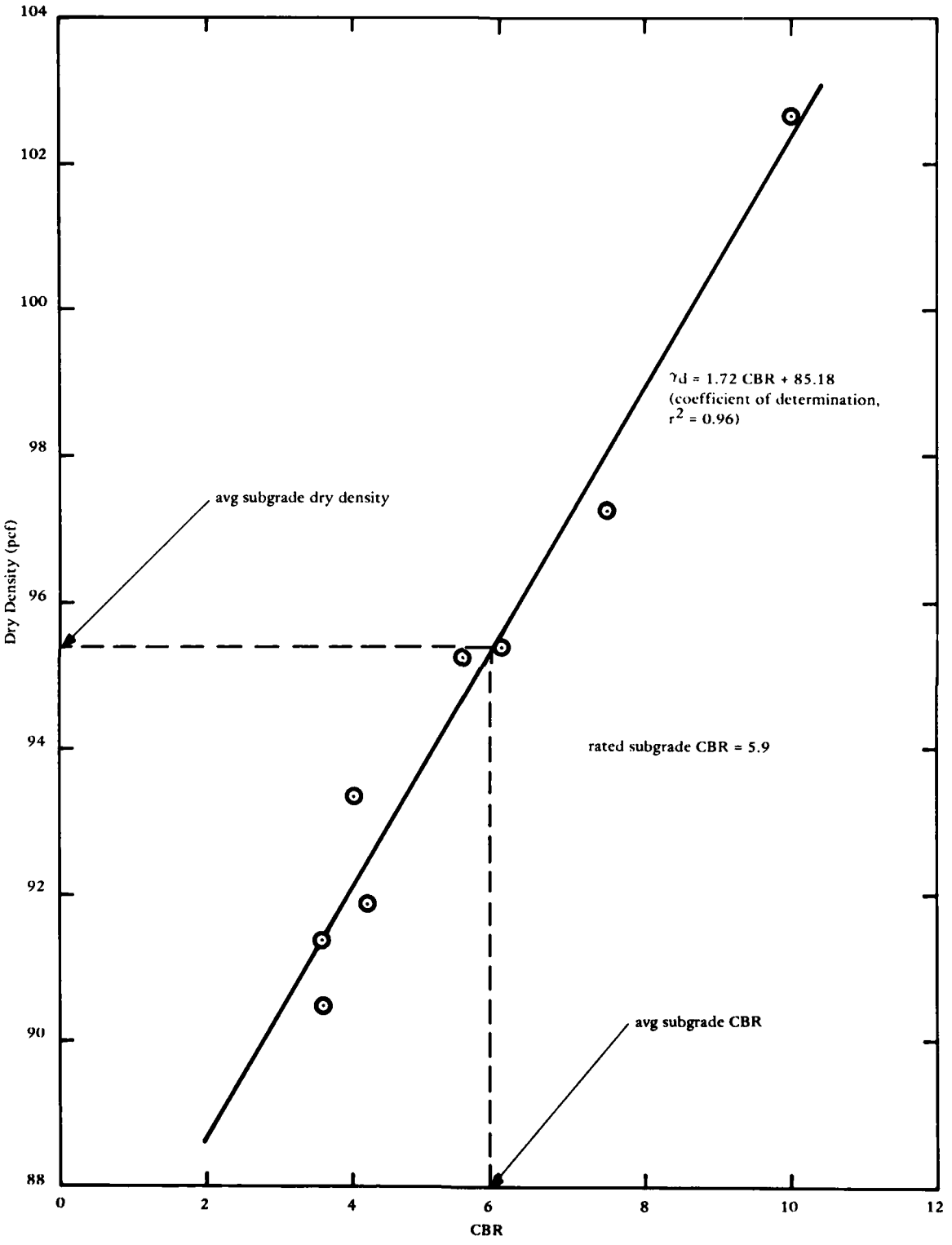

Figure 2. Wewahitchka clay CBR and dry-density relationship.

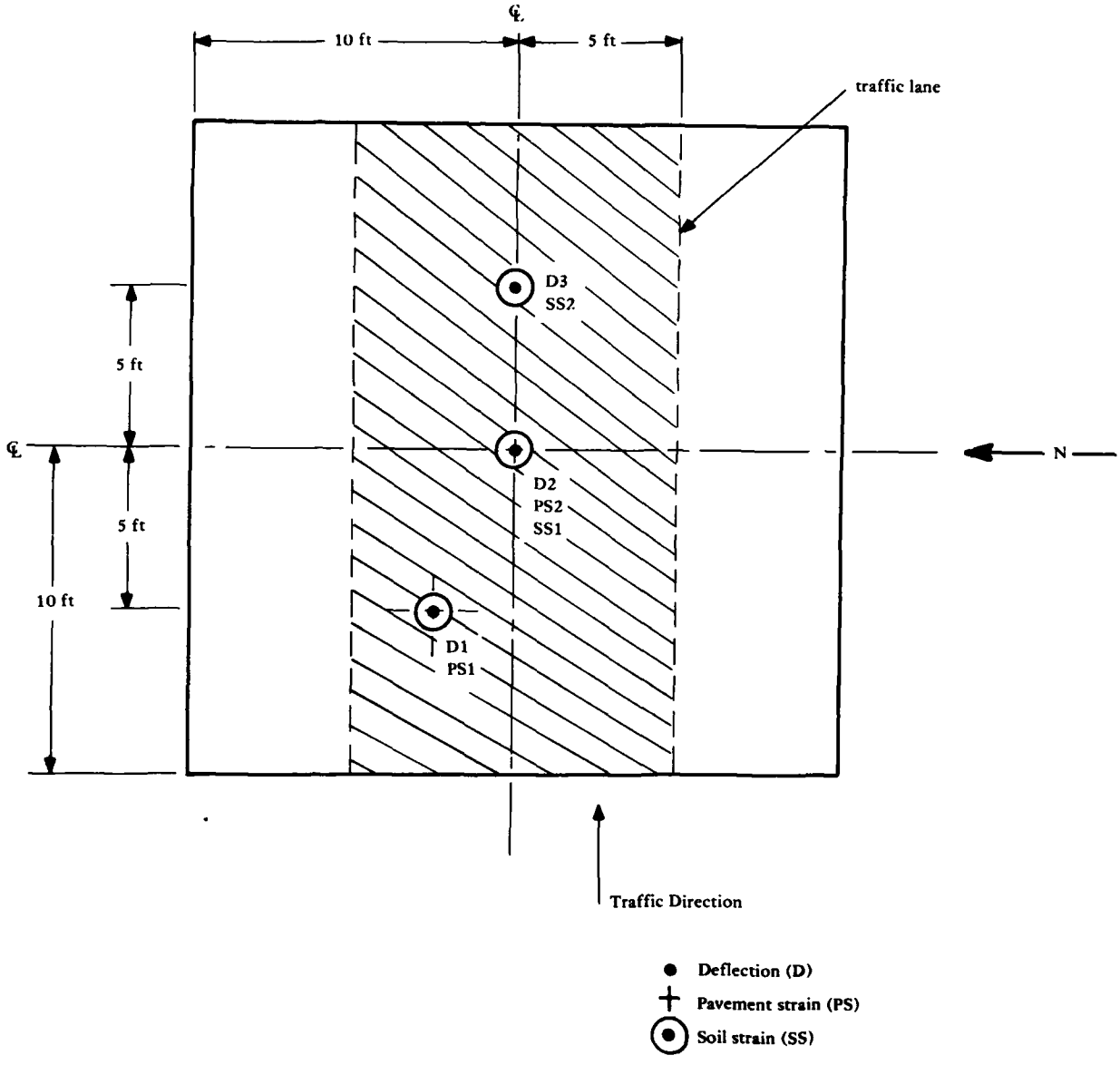

Figure 3. Instrumentation locations.

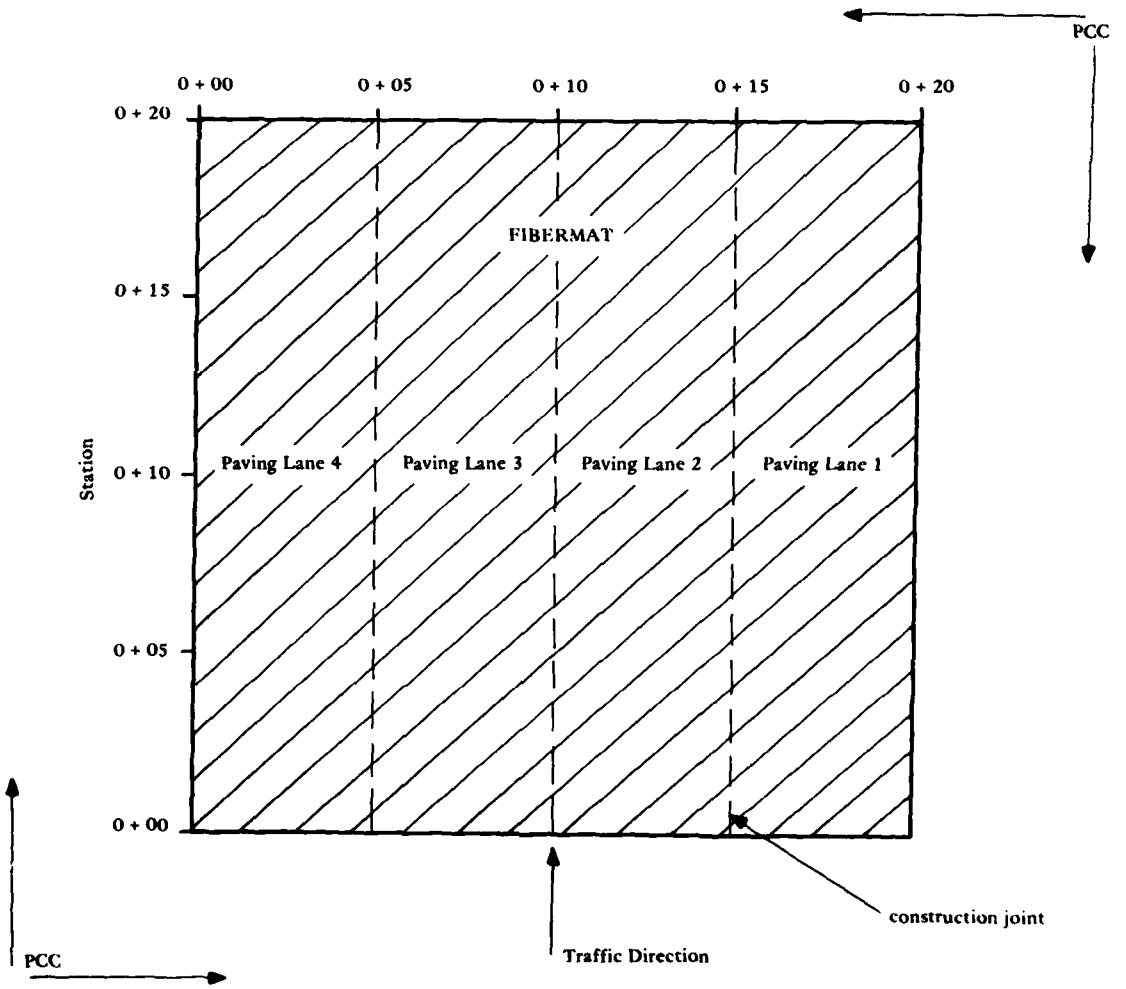

Figure 4. Paving lanes and construction joint locations.

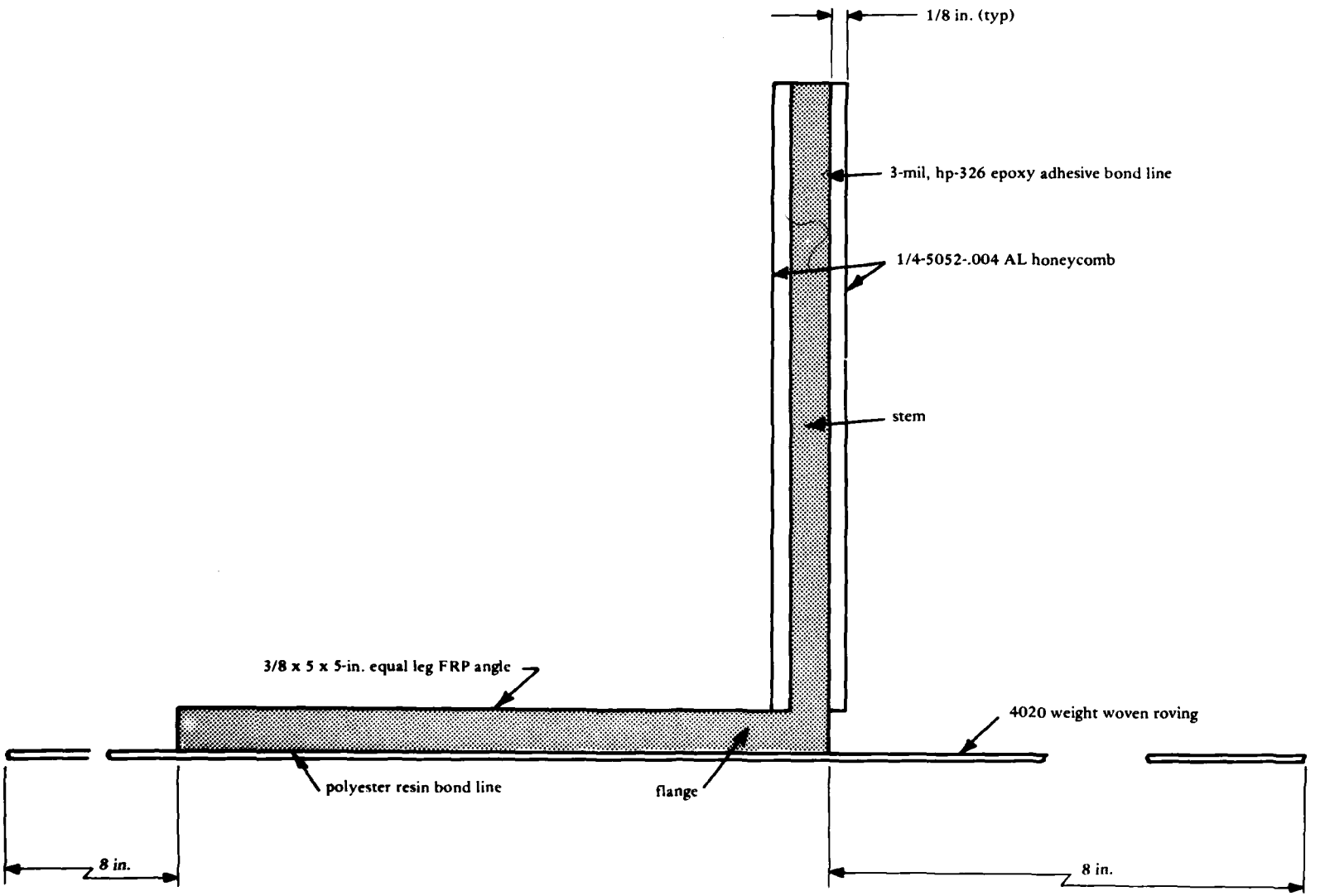

Figure 5. Fiberglass construction joint details.

(a) Construction joint.

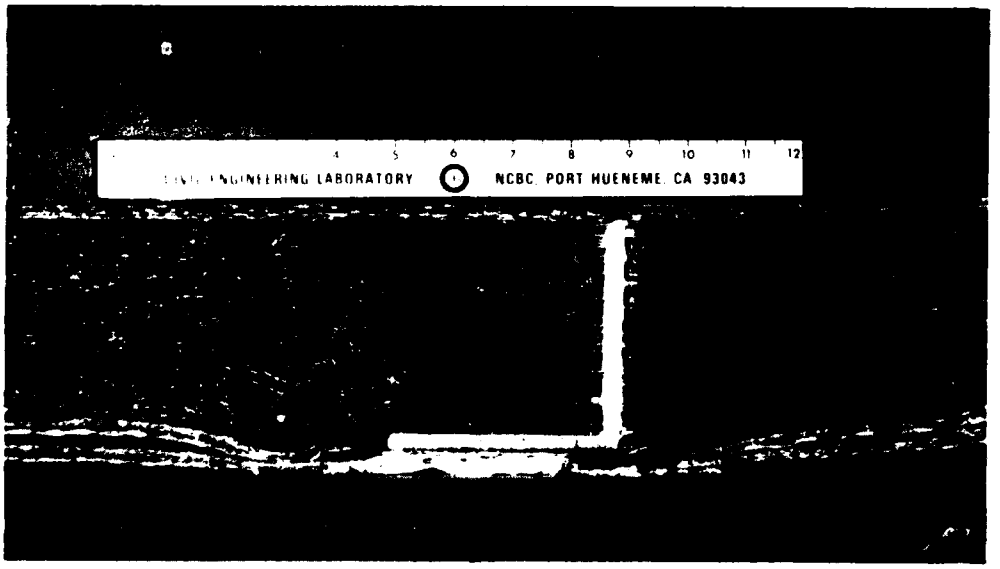

(b) Joined pavement section after load testing.

Figure 6. Typical fiberglass construction joint.

Figure 7. Spray application of fiberglass reinforced rigid polyurethane foam.

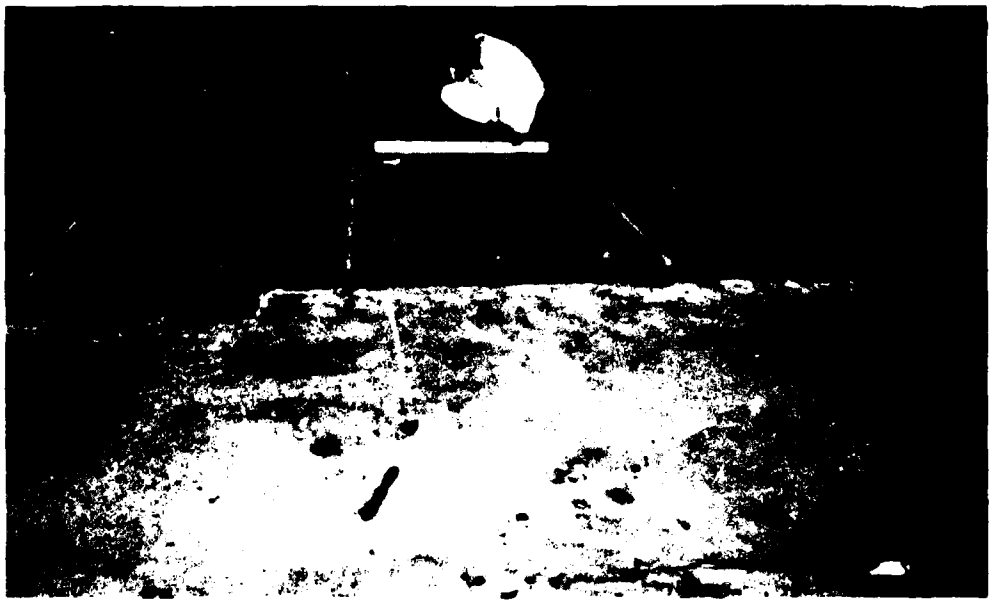

Figure 8. Trimmed polyurethane foam.

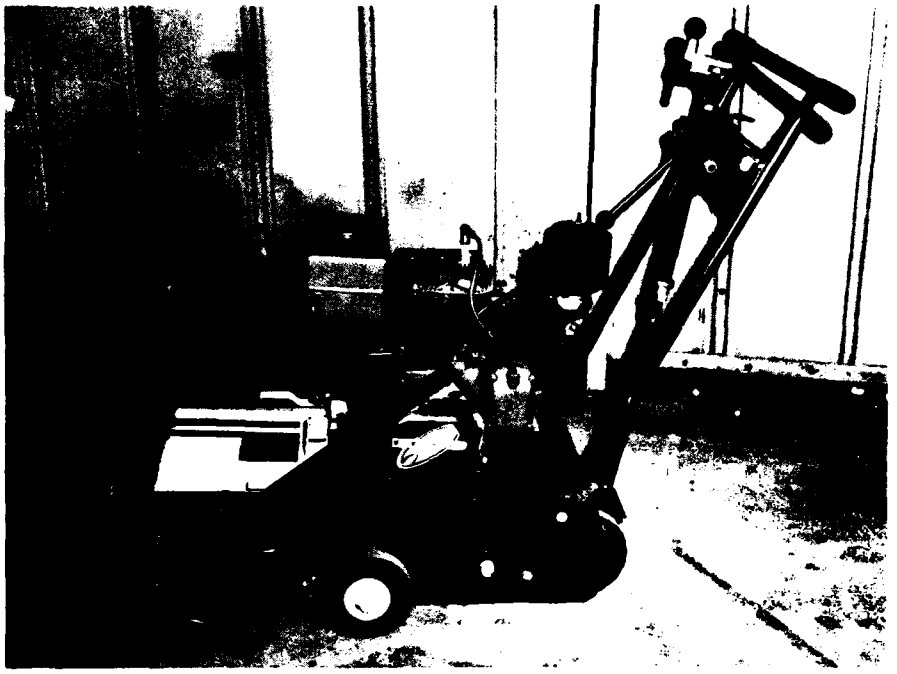

(a) Concrete planer.

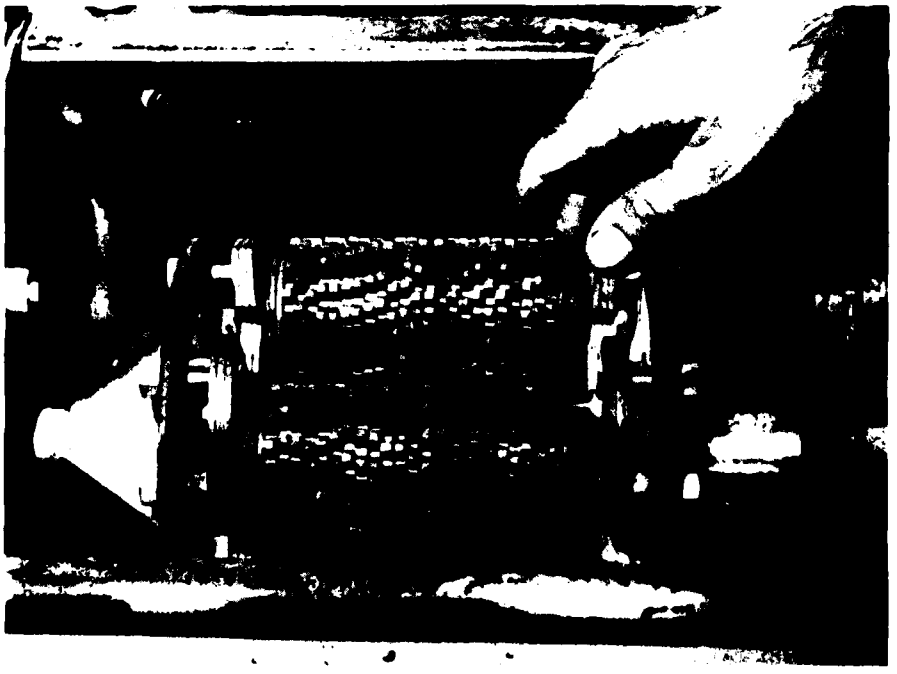

(b) Cutting blades.

Figure 9. EDCO model CP-V concrete planer.

Figure 10. F-4 load cart.

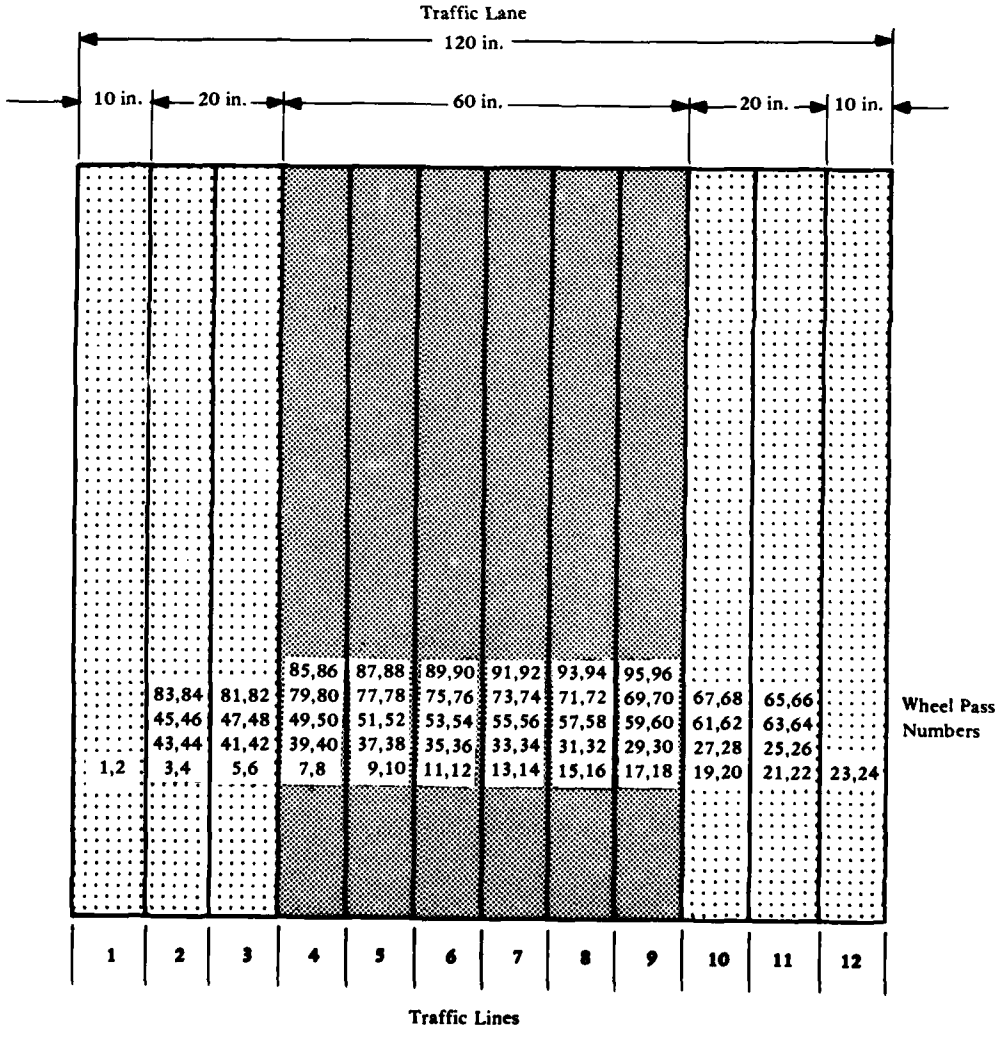

Figure 11. Traffic distribution pattern.

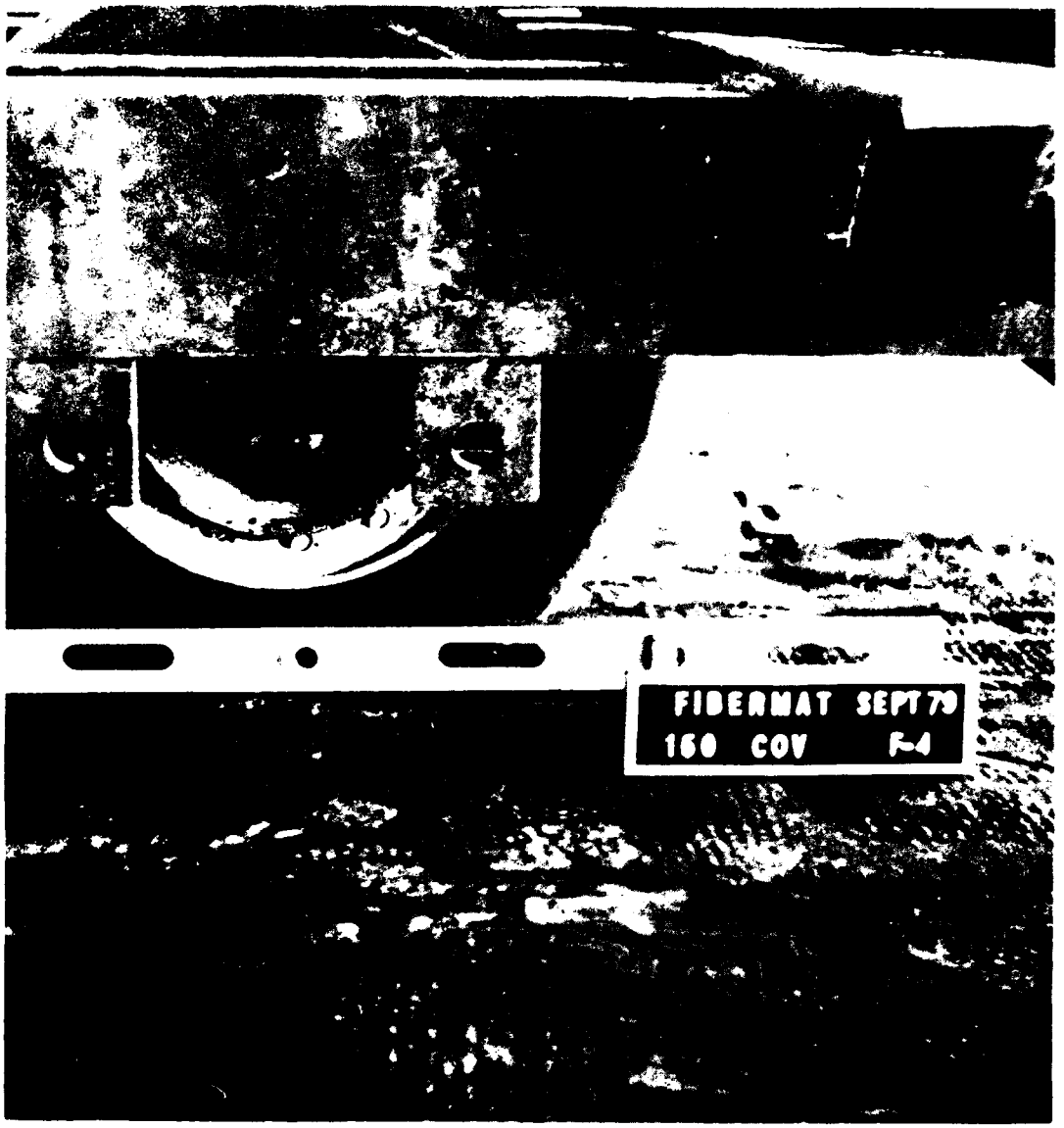

Figure 12. Elastic deflection measurement at 150 coverages.

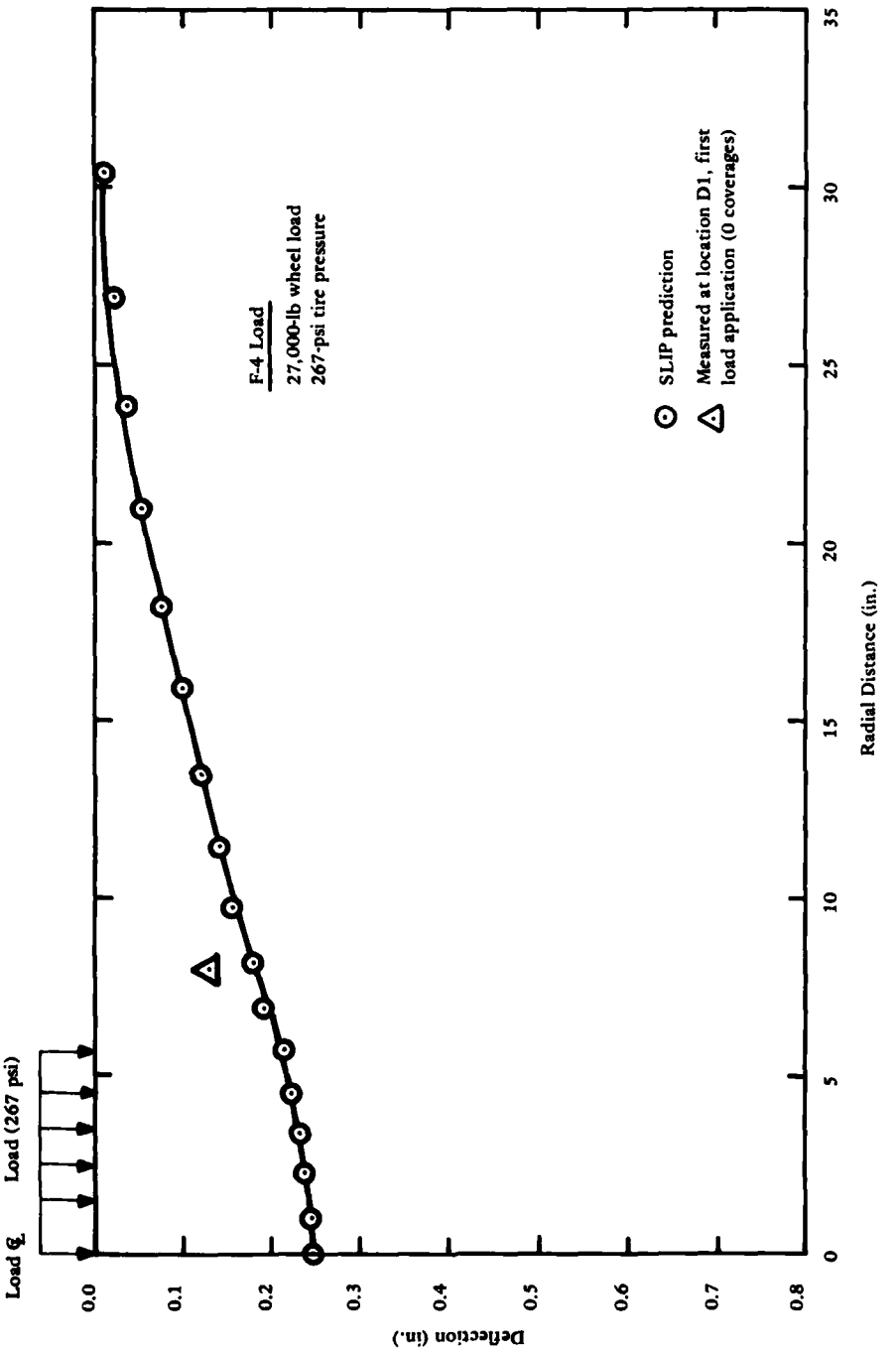

Figure 13. Predicted deflection profile and measured deflection.

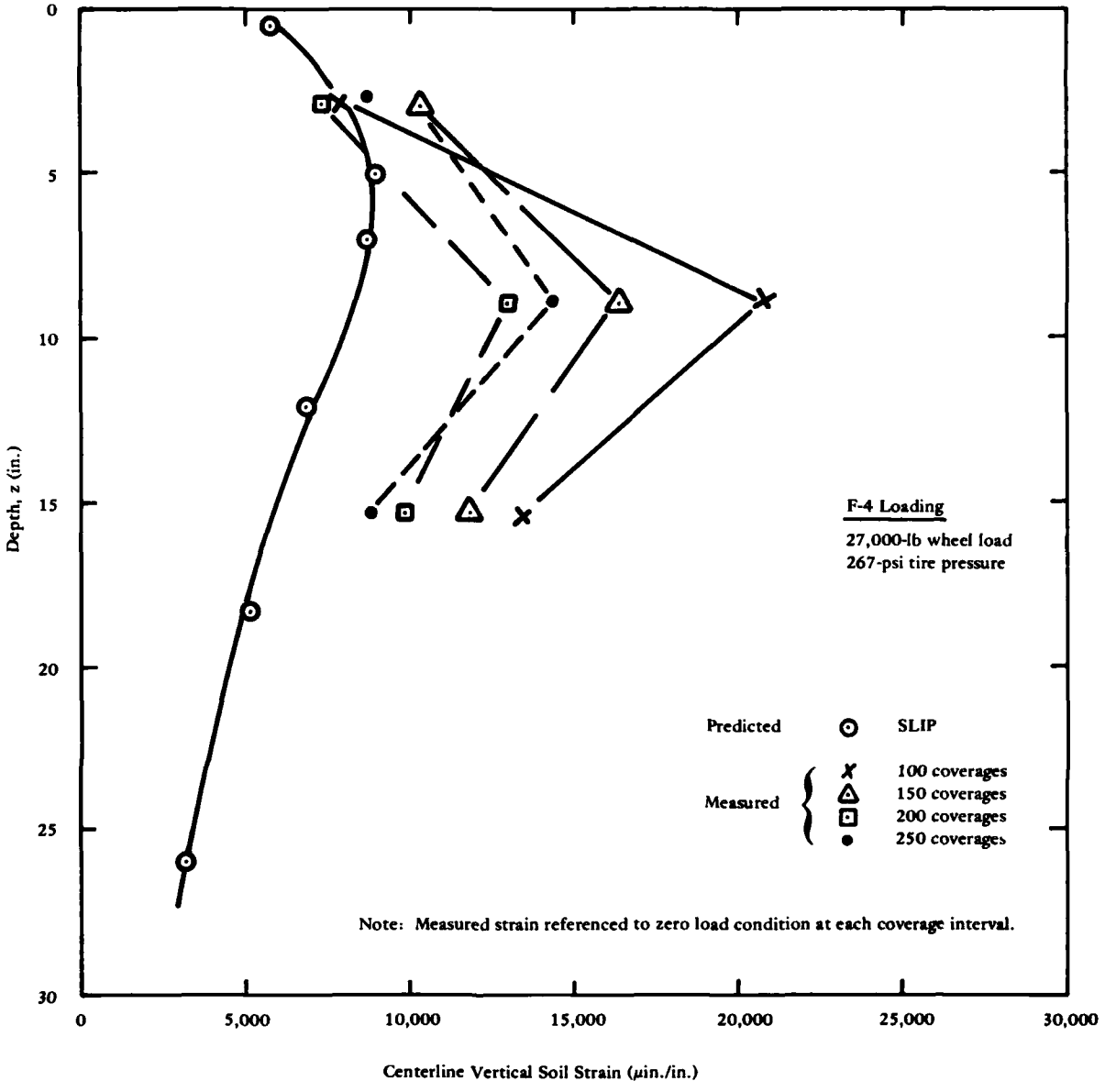

Figure 14. Measured and predicted vertical soil strain beneath load centerline.

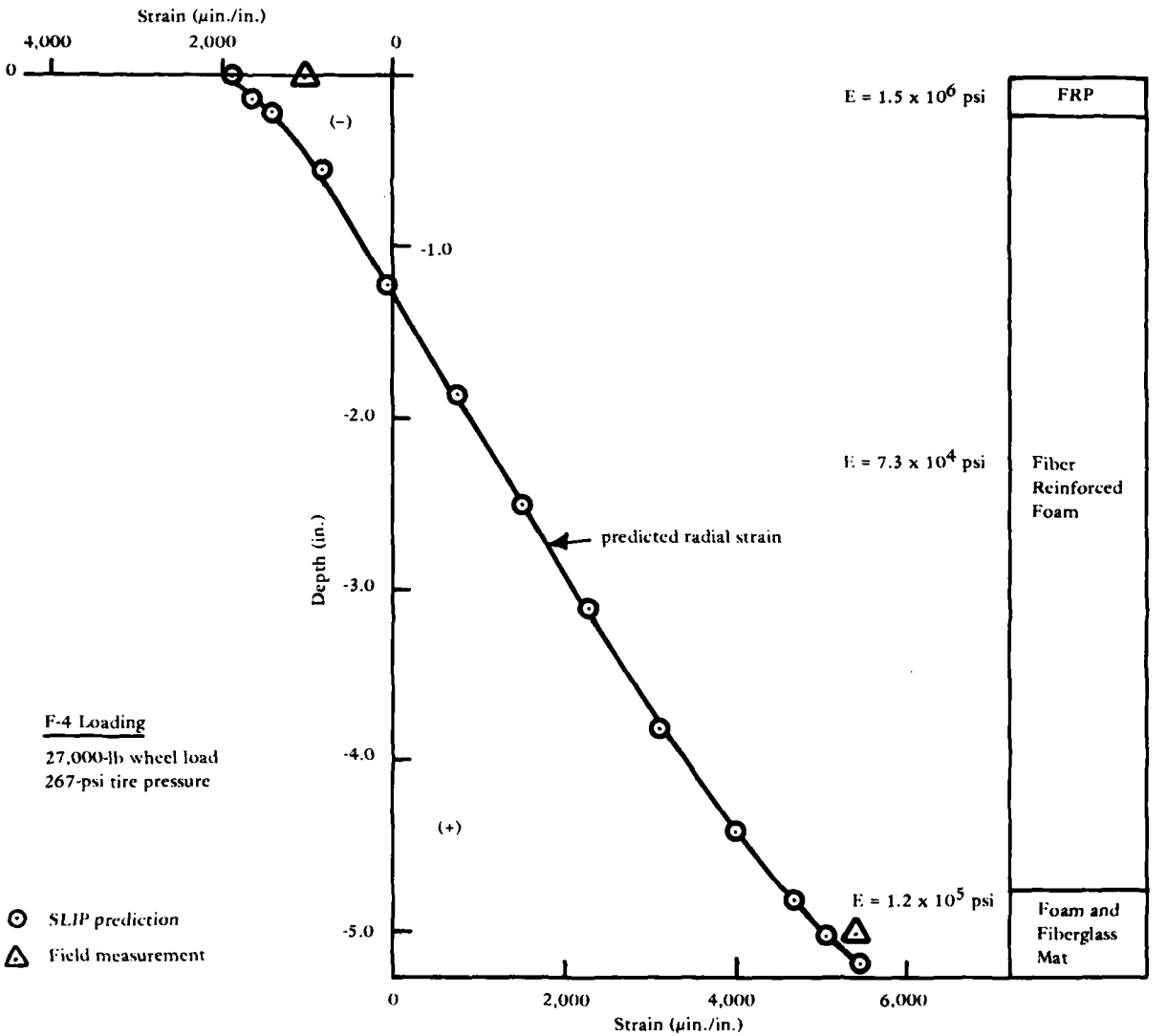

Figure 15. Predicted and measured pavement strain.

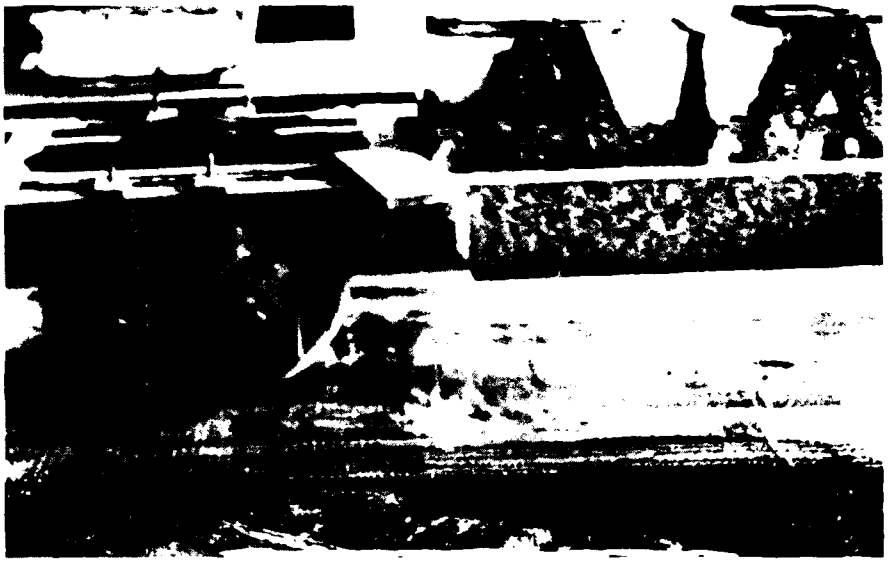

Figure 16. Load cart trafficking patch in paving lane #2.

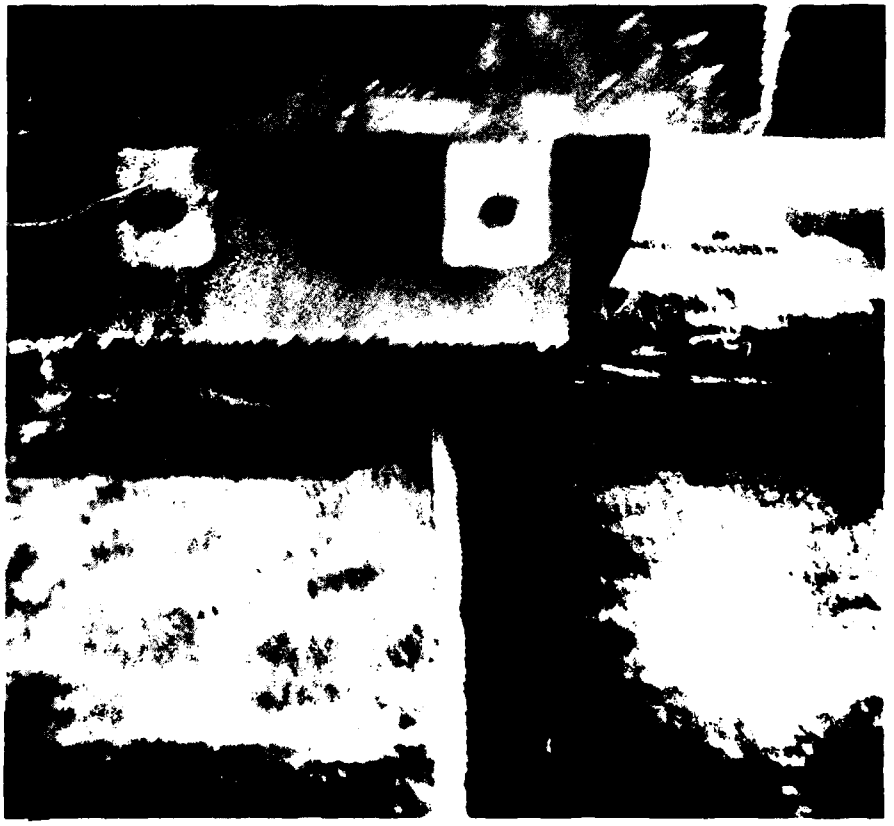

Figure 17. Arresting cable roll-over test.

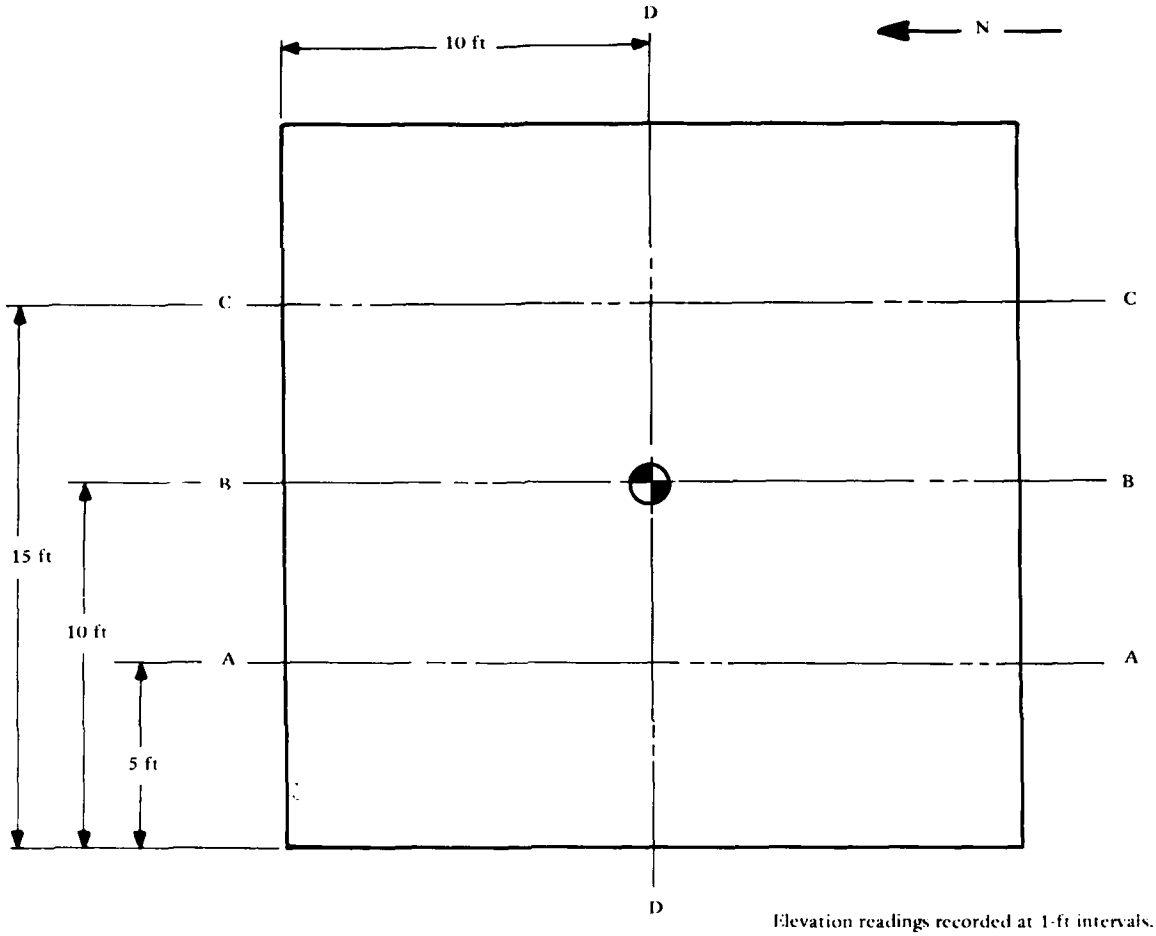

Elevation readings recorded at 1-ft intervals.

Figure 18. Survey lines.

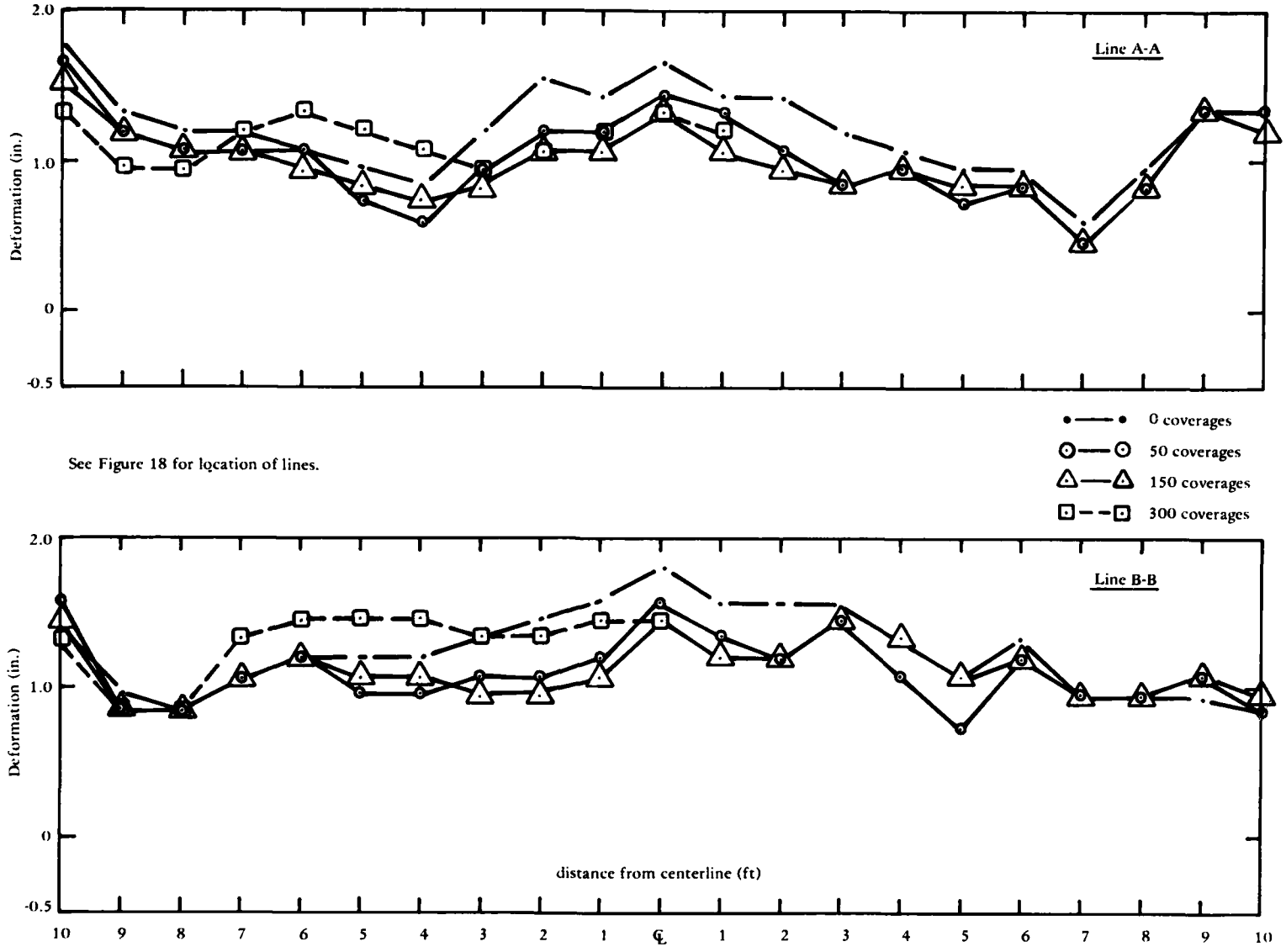

Figure 19. Profiles of pavement surface at lines A and B after 0, 50, 150 and 300 coverages.

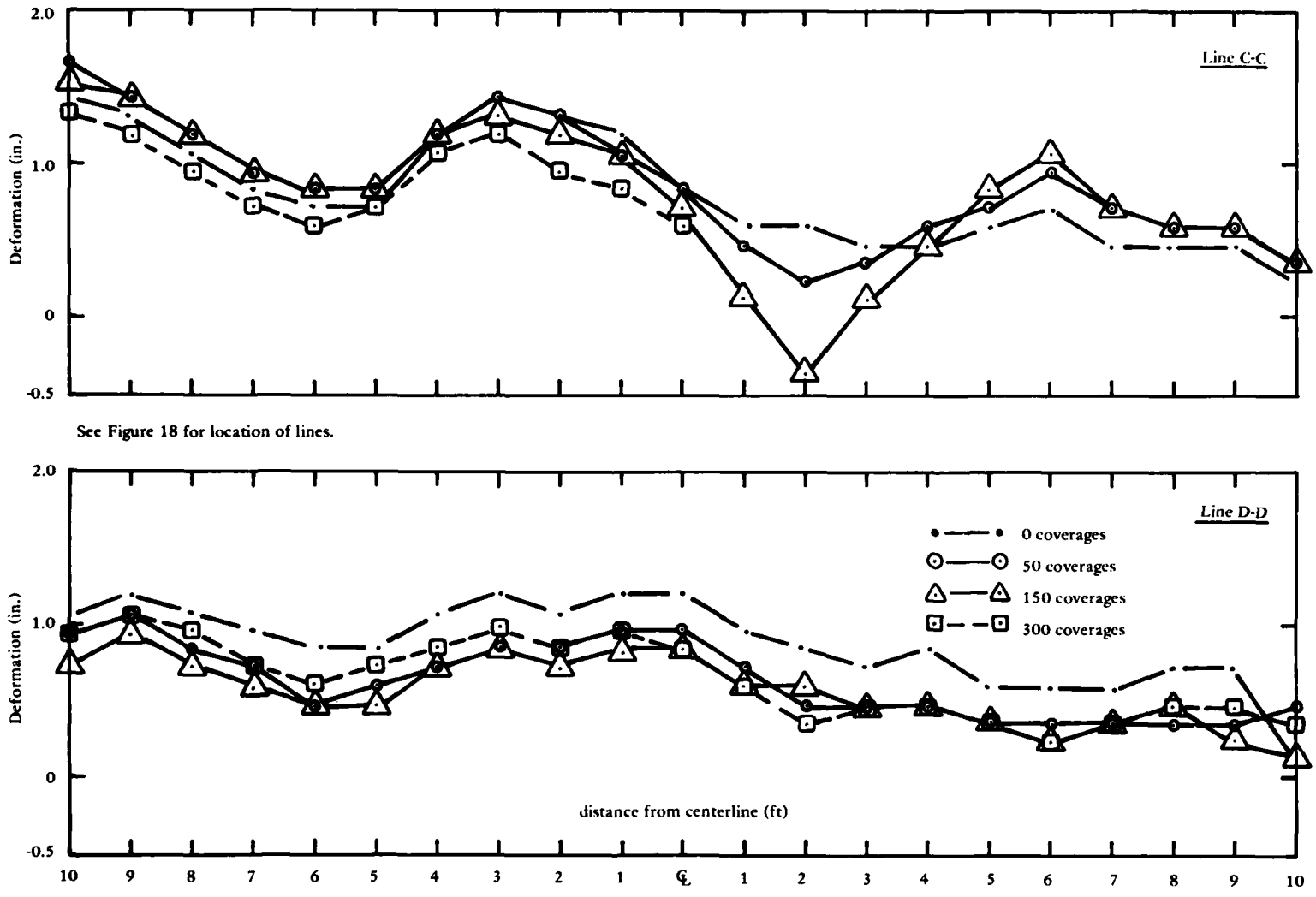

Figure 20. Profiles of pavement surfaces at lines C and D after 0, 50, 150 and 300 coverages.

Appendix A

RRR TEST FACILITY*

A permanent facility was constructed at Tyndall AFB, Fla., by the Air Force Civil Engineering Center, Directorate of Field Technology, to allow accelerated traffic tests of various pavement repair materials and designs. A clay core 60 feet wide, 220 feet long, and 6 feet deep was placed and compacted at a high water content to provide a weak test subgrade. Twelve inches of crushed limestone was placed as a base course followed by a 10-inch-thick PCC pavement. Three 20 x 20 ft sections were left open in the concrete to serve as test pits. The local dune sand was stabilized with oyster shells to construct a sand fill around the test site. The local water table fluctuates and, during wet seasons, is at approximately the surface of the natural sand subgrade.

The 20-foot test pits provide a location to construct representative pavement repairs. The depth to the clay subgrade can be varied by adding or removing clay as necessary. Following traffic on any test repair, the repair materials can be removed, and a different repair constructed in the same pit.

The test pits do not try to duplicate the crater repair problem. Because of the many variations in crater types and sizes and their very erratic geometry (Ref 15), attempts to construct model representative craters would be futile. Instead, the dimensions of the test pits were selected to provide a controlled test of the joint between the pavement and the repair and also, in the middle of the test pit, to test the repair performance over a soft subgrade with a minimum effect from edge conditions. The 20-foot dimension is also considered as the approximate point where use of a landing mat patch becomes less desirable and, though there is tremendous variation of airfield pavement slab size, it is felt to be representative of airfield slab sizes.

Portable covers were constructed to protect the test pits from rain but it was necessary to supplement these with rubber seals glued into shallow saw cuts approximately 6 inches from the edge of the test pit. A "snow fence" was also erected around the test pad to reduce problems with blowing and drifting sand. A prefabricated building is presently being erected over the site to allow testing during inclement weather.

The clay used for the test subgrade is a local clay obtained from near Wewahitchka, Fla. It is classified as CH under the Unified Soil Classification Sytem (Ref 3). Table A-1 shows physical properties and Table A-2 mineralogical composition of the clay. This clay was placed at an average moisture content of 27% and a CBR of 4. This strength was selected as a representative lower bound for crater debris backfill based on eight previous crater repair field tests (Ref 16).

*Reprinted from Reference 14.

Table A-1. Physical Properties of Wewahitchka Clay

Properties	Range	Average
Liquid Limit	57 - 79	65
Plastic Limit	21 - 30	25
Plasticity Index	30 - 52	41
Specific Gravity	2.58 - 2.67	2.61
CE-55 Opt Dry Density, pcf	110 - 115	113
Opt Moisture, %	13 - 15	14.5
CE-26 Opt Dry Density, pcf	105 - 109	107
Opt Moisture, %	13 - 16.5	14.5
CE-12 Opt Dry Density, pcf	98 - 102.5	99.0
Opt Moisture, %	11.5 - 18	15.0

Table A-2. Mineralogical Composition of Wewahitchka Clay

Mineral Constituents	Relative Sample Contents
Clay	
Kaolinite	Intermediate (25%-50%)
Smectite	Common (10%-25%)
Clay-mica	Common (10%-25%)
Non-clays	
Quartz	Intermediate (25%-50%)
Feldspars	Rare (>5%)

Appendix B

BENCH MODEL FOAM MIXING EQUIPMENT

A bench model two-component resin mixing and dispensing system (Figure B-1) was designed and fabricated under contract with Johnson and Sons, Glendale, Calif. The system is designed to mix and spray a two-component rigid polyurethane foam - CPR 739, 20-pcf density foam manufactured by the CPR Division of the Upjohn Co., Torrance, Calif. The foam component characteristics are presented in Table B-1.

The two 452TB model series, double-acting piston, positive displacement pumps of the spray system were fabricated by the Grover Manufacturing Corporation, Montebello, Calif., and are capable of delivering the mixed polyurethane foam at a rate of 30 lb/min. The system requires a 50-cfm air supply at 100 psi pressure. The two resin pumps are mechanically coupled with a rack-and-pinion gear arrangement for precise control of component ratio at 54 parts of component A to 46 parts of component B by volume. One of the pumps is slaved to the other with the master pump having a pilot head which controls the cycling of the pumps by alternately directing air to the top or bottom of the air pistons to drive them down or push them up.

A static-type mixing element (Figure B-2) mixes the resin components by splitting and recombining them hundreds of times as they are forced through the 15-inch-long mixing barrel of the spray gun. The spray gun (Figure B-3) also features a Johnson model J-2 fiberglass roving chopper connected to a 1-inch-diam by 18-inch-long stainless steel tube. Glass roving chopped into fibers 1/4 inch to 1 inch long is blown through the tube into the foam spray pattern, thereby intimately mixing the foam and chopped fiberglass. The glass quantity is determined by the speed of the cutter and is varied by regulation of air flow to the cutter.

Two hoses carrying the component materials from the pumps to the spray gun remain in a "wet" condition between jobs and are rinsed with solvent only prior to prolonged storage. A separate hose circuit runs from an air-pressurized (30-psi) solvent tank to the spray gun mixing chamber to efficiently clean the mixing chamber and spray nozzle with minimal solvent usage (approximately 1 quart).

Table B-1. CPR-739 Rigid Polyurethane Foam Component Characteristics

[Cream Time, 120 sec; Rise Time, 13 sec; Cure Time, 24 hr at 75°F.]

Temperature (°F)	Viscosity (cP/s)	
	Component A	Component B
70	3,500	3,600
80	1,800	2,000
90	1,100	1,200

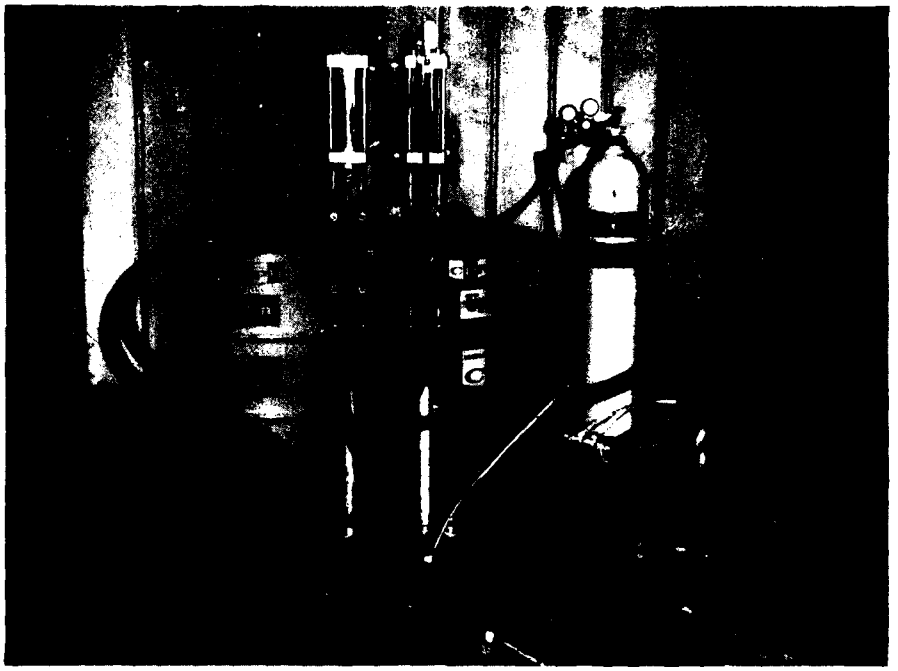

Figure B-1. Bench model two-component polyurethane foam spray machine.

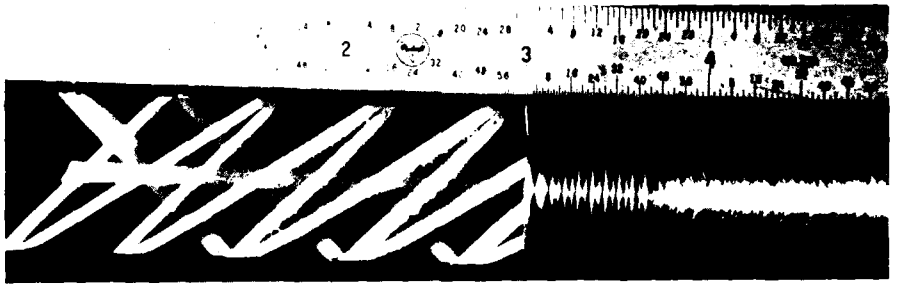

Figure B-2. Static mixing element.

Figure B-3. Polyurethane foam spary gun.

Appendix C

SOIL TESTING AND STRUCTURAL ANALYSIS

SOIL TESTING

Samples of the heavy clay soil (Wewahitchka clay) used in rapid runway repair (RRR) testing at Tyndall AFB, Fla., were obtained from the Research Division of the AFESC. The clay was received at a moisture content of 42% (by weight) and allowed to air dry until moisture content had lowered to approximately 28%. The sample was then thoroughly mixed to insure uniformity and placed in a sealed container to prevent moisture loss. Samples were prepared for triaxial shear testing using a 2.8-inch-diam mold. Samples were compacted by hand-tamping into the mold in five equal layers. The soil for each layer was weighed and layer height controlled to give a compacted density equal to a pre-determined density which corresponded to that of the clay in the Tyndall subgrade. Nominal clay density, water content, and sample height were 95 pcf (dry density), 28% by weight, and 6 inches, respectively.

In consideration of the rapid nature of the loading which would be produced by the moving wheel load of the test cart and the impermeability of the clay, unconsolidated-undrained triaxial tests were conducted. Samples were prepared and tested at a moisture content corresponding to that of the Tyndall subgrade, and thus were not in a completely saturated condition at start of the triaxial tests. The test apparatus was a CKC e/p cyclic loader developed by Dr. Clarence Chan, research engineer and lecturer of the University of California at Berkeley. Each sample was subjected to a confining pressure and, with cell drainage lines closed, immediately (2 to 4 minutes) loaded at a rate of approximately 5 psi/min. Samples were tested to failure at three different confining pressures. Plots of soil response are presented in Figure C-1, and the Mohr failure envelopes are depicted in Figure C-2. The shearing strength of the clay is represented by the cohesion since the test circumstances resulted in the $\phi = 0$ condition.*

*The pore pressure of a saturated cohesive sample triaxial tested in an undrained condition acts with equal intensity in all directions; thus, the increment of pore pressure is the same for both major and minor principal stresses. The failure circle for each test has the same diameter whether it is plotted in terms of effective stresses or total stresses. If several samples are tested under undrained conditions at different cell pressures, the rupture line with respect to total stresses (Figure C-2) is horizontal.

Although not completely saturated, the tested samples of Wewahitchka clay were compacted at above optimum moisture content (27% versus 17%) with a degree of saturation of 94%. This high degree of saturation led to performance of the clay as, essentially, a saturated sample. Previous research conducted on not fully saturated clays compacted at above-optimum moisture content has indicated a horizontal failure envelope for triaxial tests conducted on samples in an undrained condition and at confining pressures up to 1,000 psi (Ref 17).

STRUCTURAL ANALYSIS

A finite element computer code SLIP, developed by E. L. Wilson of the University of California and later modified by CEL (Ref 8), was used to predict, before trafficking, the performance of the FIBERMAT pavement. In general, SLIP models a pavement system as an axisymmetric solid (layered conical frustrum) and is based upon elastic layered assumptions with solution by the finite element technique. Infinitely small strain, small displacement theory, and linear elastic material response are critical assumptions of the method.

The idealized pavement-soil system used for the analysis is illustrated in Figure C-3. The program was flagged to include tangential slip (frictionless behavior) at the pavement-soil interface and to solve for the condition of boundaries free at an angle of 30 degrees to the vertical. An F-4 aircraft main gear wheel load was input as a pressure loading of 267 psi over a 5.67-inch radius. Total system (soil and pavement) depth was fixed at 15 load radii, and width was held constant at 6 radii. Seventeen radial elements were specified; and three, seven, and three element rows were specified for the FRP, fiber-reinforced foam, and mat-reinforced foam sections of the FIBERMAT pavement, respectively (Figure C-3). The program was flagged to generate an optimum number of elements for the soil.* Elastic moduli for the foam sections of the FIBERMAT pavement were determined from quasi-static flexure tests previously conducted on beams of the representative materials (Ref 1). The elastic modulus for the FRP was derived from tension tests (Ref 18) and is considered representative of the elastic modulus in compression.

An elastic modulus was estimated initially for the clay and input to the computer program. An iterative procedure was then employed whereby the computer-predicted soil stress state (at a depth of one load radius within the subgrade**) was located on the soil stress-strain curve, and the elastic modulus was computed at the point, using the secant method (Figure C-4). The new modulus was then input to the computer program, and the code was re-run. This sequence was iterated until experimental soil moduli and stress states (from Figure C-4) matched those for the representative element of the SLIP pavement system model. The degree of matching between the analytical and experimental soil stress states which were used to characterize the material models for analysis can be reviewed in Table C-1. The final predicted stress state was marked on the material response curve (Figure C-4). It should be noted that the original assumption of linear-elastic soil behavior was not seriously in error as the clay response at the given stress level was approximately linear-elastic.

*Previous analyses have confirmed the foregoing to be an economical mesh configuration which satisfies convergence criteria.

**Analyses of full-scale laod tests conducted by CEL have indicated that, for loads placed directly on dense sand and clay subgrades, the stress state which appeared to be representative of the average state for the subgrade was that located at a depth of one load radius beneath the load center (Ref 19).

The final estimate of initial static deflection beneath the F-4 wheel load was 0.25 inch, and the deflection profile is presented as Figure 13. The predicted soil strain distribution beneath the load centerline is plotted in Figure 14 and pavement strain in Figure 15.

Table C-1. Soil Stress State at z = 10.29 inch[c]

Parameter[a]	SLIP Prediction[b]	Experimental Curve[b]
E	1,047 (input)	1,047
σ_z	-12.9	-9.5
σ_r	-4.4	-5.0
Σ_z	-0.90	-0.90

[a] z = depth below load surface, in.
σ_z = vertical normal stress, psi
σ_r = radial normal stress, psi
ε_z = vertical (axial) strain, μin./in.
E = elastic (Young's) modulus, psi

[b] Minus indicates compression.

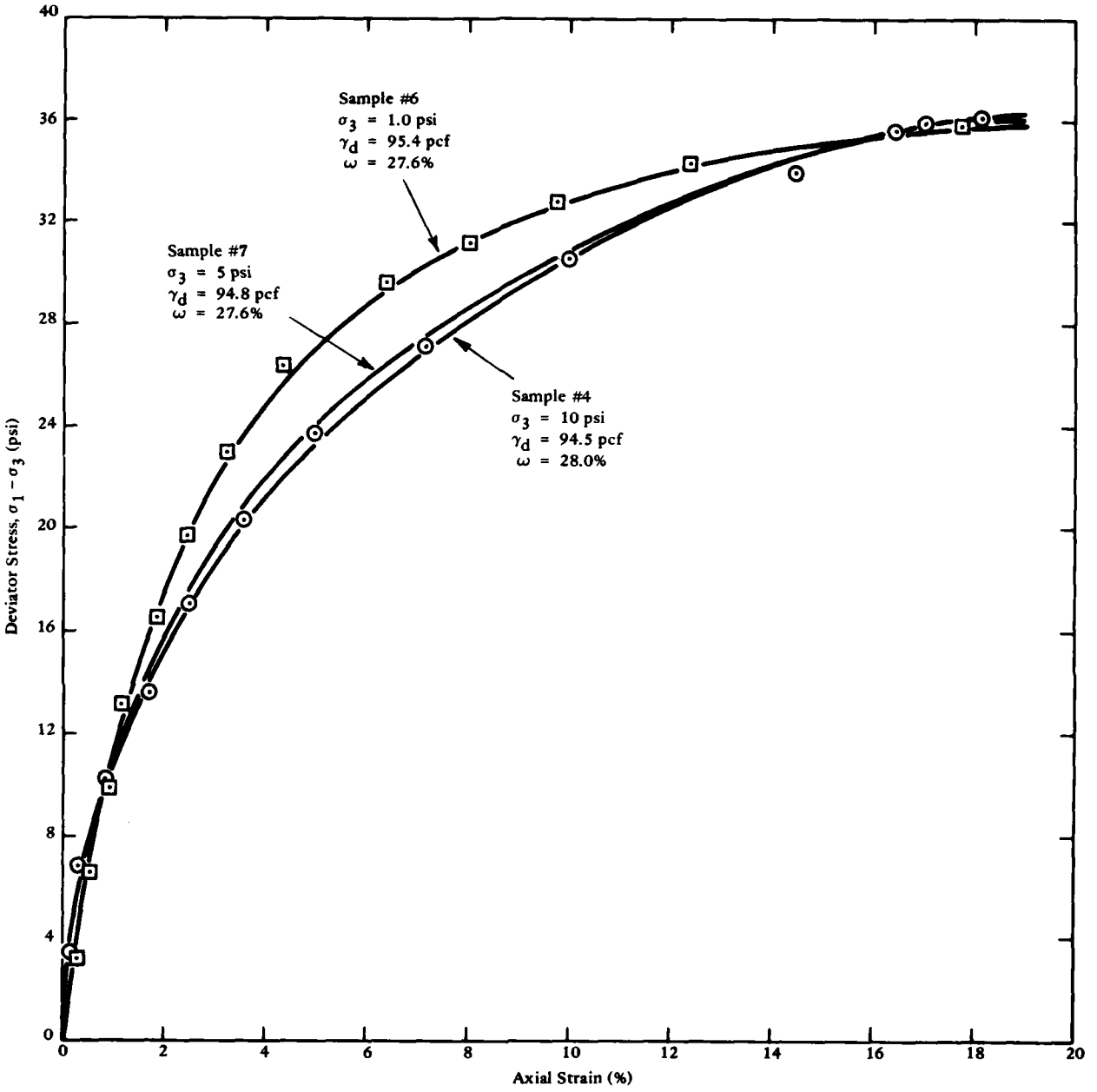

Figure C-1. Response characteristics of Wewahitchka clay triaxial tested in an unconsolidated-undrained condition.

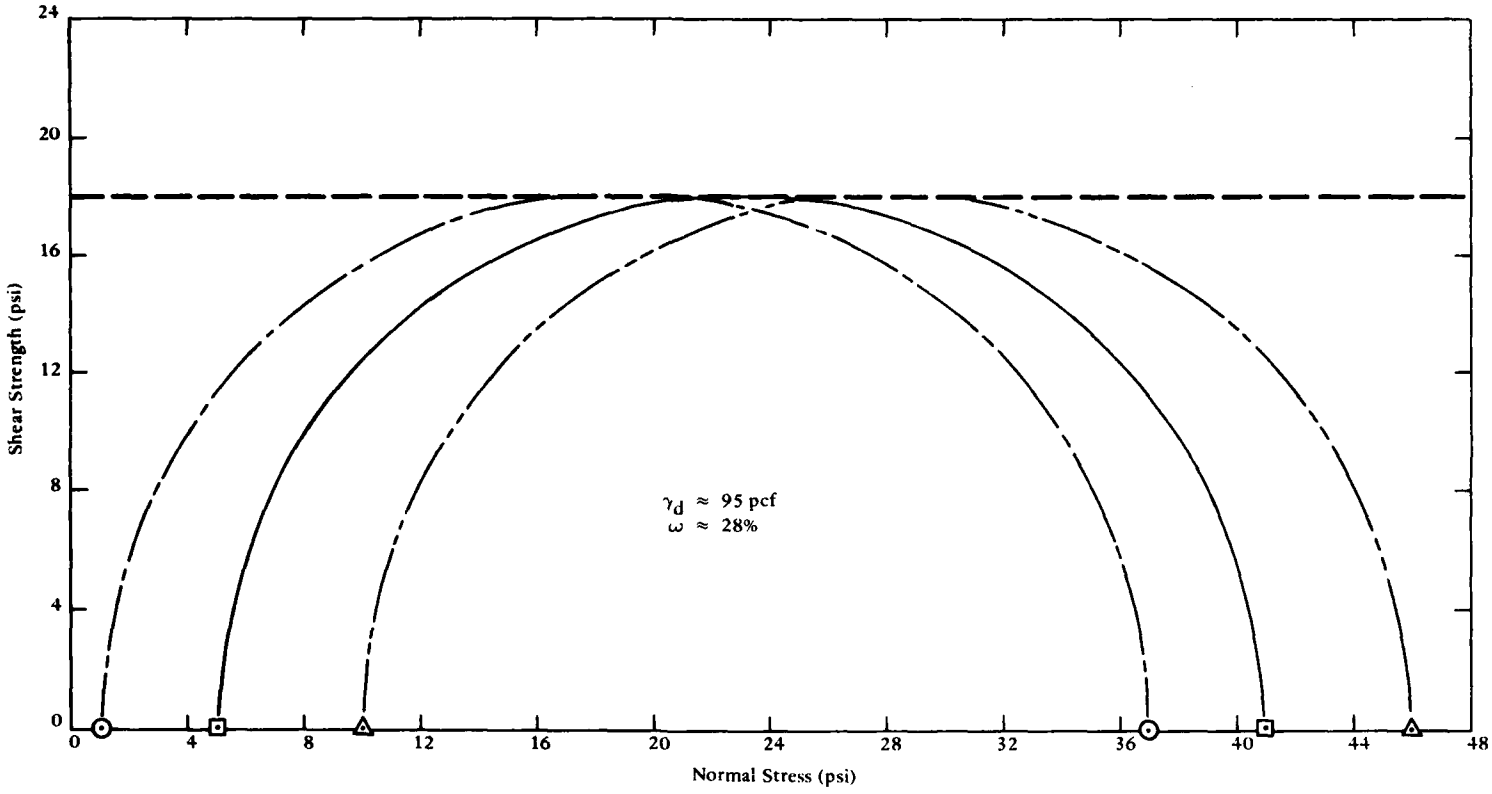

Figure C-2. Failure envelopes for Wewahitchka clay triaxial tested in an unconsolidated-undrained condition.

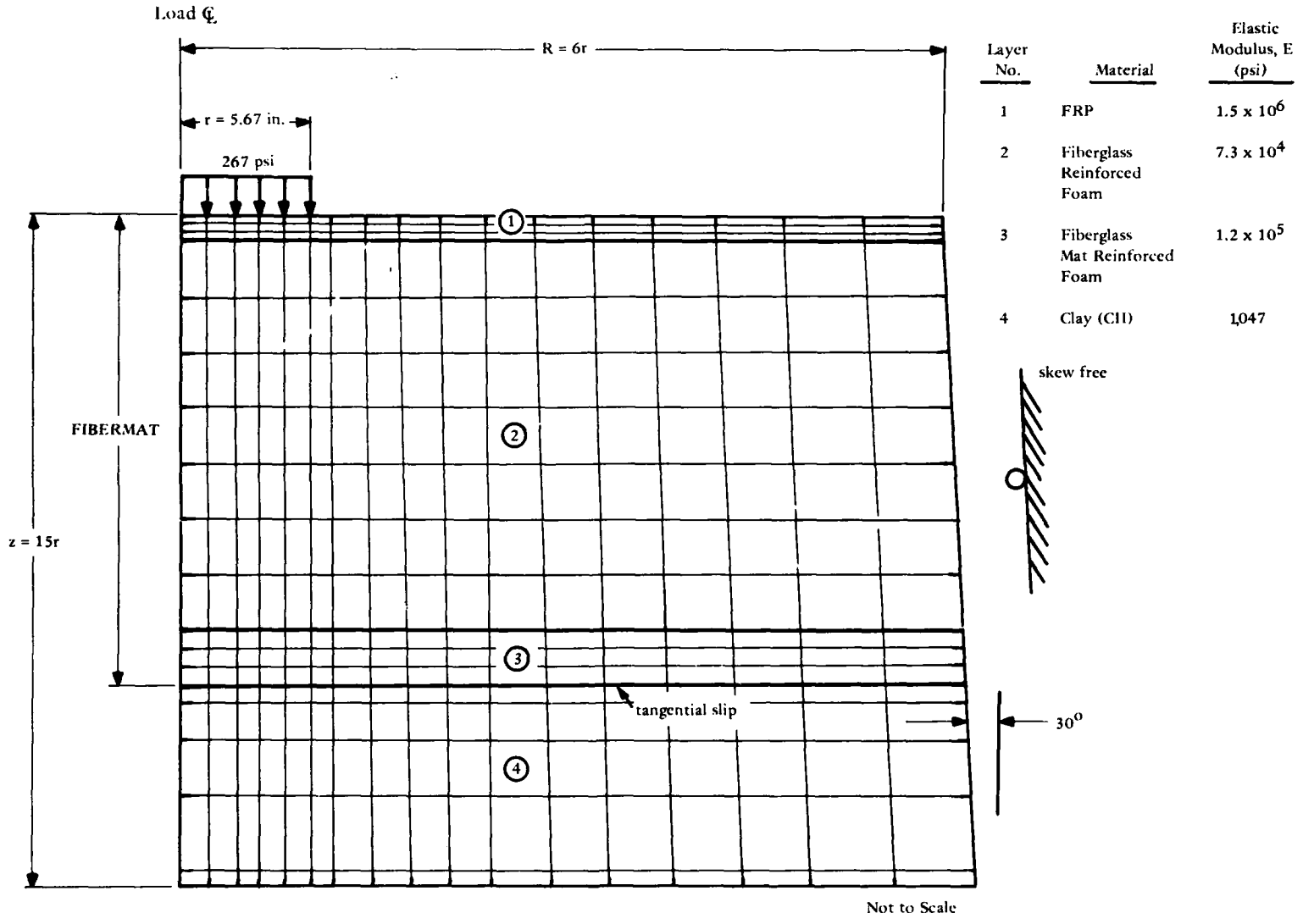

Layer No.	Material	Elastic Modulus, E (psi)
1	FRP	1.5×10^6
2	Fiberglass Reinforced Foam	7.3×10^4
3	Fiberglass Mat Reinforced Foam	1.2×10^5
4	Clay (CH)	1,047

Figure C-3. Idealized FIBERMAT pavement and soil system.

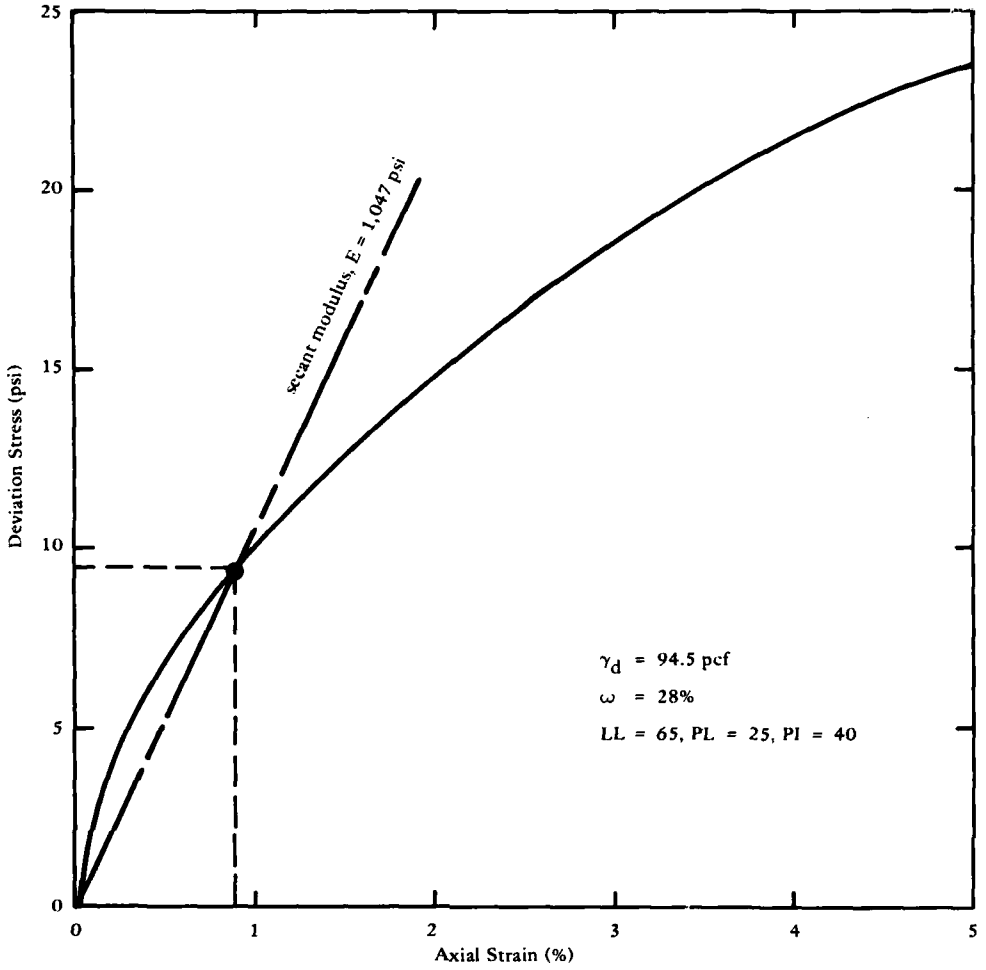

Figure C-4. Averaged response for Wewahitchka clay triaxial tested in an unconsolidated-undrained condition.

Appendix D

PAVEMENT DESIGN AND LOGISTIC ANALYSIS

After the traffic testing, analyses were conducted to predict the weight, material cost, and cube logistic factors for an EAF constructed on a subgrade having a strength indicative of a CBR of 10. Pavement sections were designed to satisfy the critical load parameters for the various EAF traffic areas. A similar design was completed during FY77 (Ref 1) when EAF traffic areas were defined and safety factors (Table D-1) were assigned on ultimate pavement stresses. The safety factors were based primarily upon engineering judgment with consideration of traffic quantity, type of traffic, load nature, fatigue data, and criticality of the traffic area with respect to the operation of the EAF. The completion of the first traffic test of FIBERMAT has afforded an opportunity to review these factors of safety.

Data gathered during the traffic testing have indicated that the pavement-soil system performed essentially as predicted by the computer program, SLIP, for an initial static loading. The eventual failure of the pavement was caused by intensification of flaws formed within the pavement during construction. Since the pavement section was constructed with bench model - not prototype - equipment, a modification of safety factors to offset construction defects is not currently recommended. Given the limited available performance data, the factors of safety are considered appropriate, and a change at this time is unwarranted.

Table D-1. Safety Factors for FIBERMAT Surfacing Design

Traffic Area	Factor of Safety
Runway	
Centerline (Area C1)	3.0
Edges (Area C)	3.0
Impact (Area D)	
Compression	1.1
Bending	1.5
Parking Apron	
Medium Duty (Area A)	a
Light Duty (Area B)	a

[a]Defined by limiting soil strain.

A concept for RRR using prefabricated FRP membranes as trafficable crater caps was traffic-tested concurrently with FIBERMAT (Ref 20). The success of the FRP as a trafficable surfacing for the F-4 aircraft demonstrates the feasibility of exclusively using FRP for the surfacing of an EAF parking apron for both medium and light-duty aircraft. Previously the FRP was recommended only for surfacing of the light-duty parking area (Ref 1). Accordingly, the current logistic analysis considers the parking apron to be surfaced entirely with an FRP membrane.

EAF TRAFFIC AREAS

Traffic area delineation within an expedient airfield (EAF) has been given further evaluation as a result of the success of an FRP membrane in supporting simulated F-4 aircraft traffic and after review of F-4 aircraft arrestment procedures. A landing on a conventional runway may employ either of three basic arrestments depending on required turnaround time and weather and field conditions (Ref 21). For an arresting gear located at midrunway, the arrestment types are:

1. Midfield. Touchdown immediately prior to the pendant with engagement at approximately 150-knot CAS* (depending on gear type). This procedure would be favored where poor runway traction, heavy cross winds, or other directional control problems exist.
2. Modified Midfield Arrestment. Touchdown 500 to 1,000 feet in front of the gear and engagement of the wire at approximately 135-knot CAS.
3. Long Field Arrestment. Touchdown at end of runway and roll into the arresting wire at reduced speed.

A sink rate of 600 to 700 ft/min. (10 to 11.7 ft/sec) is common for each arrestment since a constant glide slope approach to touchdown is followed using a mirror or Fresnel lens landing aid. For an EAF, therefore, touchdown could occur anywhere from each end of the runway to the two arresting gears which are located at the center of the 4,000-foot-long runway. Thus, the area subject to landing impact is not necessarily within 1,000 feet of the arresting gears as originally defined (Ref 1).

EAF traffic areas have been refined as follows to reflect both increased usage of FRP and F-4 arrestment procedures.

1. Traffic Area A. An area within the parking apron for slow moving aircraft having ESWL <30,000 pounds and with tire pressures less than 350 psi. The type A traffic area is suitable for F-18, F-14, F-4, and A-6 aircraft and is surfaced with FRP.
2. Traffic Area B. A portion of the parking apron only receiving traffic from slow-moving aircraft having ESWL <15,000 pounds and with tire pressures less than 200 psi. Traffic area B is

*Calibrated airspeed.

suitable for A-4, AV-8, and C-130 aircraft.* This area also includes the extension of runway width provided for tape runout in the vicinity of the arresting gears. Traffic area B is surfaced with an FRP membrane.

3. Traffic Area D. The portion of the runway subject to the touchdown of aircraft and thus dynamic, impact loading. This area is considered as extending from the end of the runway to each arresting gear and is 30 feet in width. The width of traffic for the F-4 aircraft is calculated as 7.4 ft.** With a tread of 17.9 feet, 75% of runway traffic would occur within the 12.7 feet to either side of the runway centerline (center 25.4 ft of the runway). The flight manual (Ref 23) for the F-4J aircraft lists 10 feet as the maximum off-center distance for engagement of an M-21 arresting gear. Consideration of the 25-foot lateral wander width and the 20-foot width derived from the specification for maximum offcenter engagement led to the conservative adoption of a 30-foot design width for traffic area D. The pavement within this area is designed for a maximum sink rate of 1,020 ft/min. (17 ft/sec).

4. Traffic Area C. The remaining 35.5 feet of runway width to each side of traffic area D. Traffic area C receives <25% of runway traffic. Pavement within this area is designed to withstand landings of the F-4 at sink rates less than 930 ft/min. (15.5 ft/sec).

5. Traffic Area C1. The center 25 feet of runway located between the two arresting gears. The pavement design is identical to that of traffic area C except that an additional layer of 4020weight fiberglass mat is included in the FRP facing for increased resistance to arresting hook impact and abrasion.

These traffic areas are delineated in Figures D-1 and D-2.

Design aircraft loads for the various traffic areas are given in Table D-2. The analyses of pavement sections were conducted with the aid of the finite element computer code SLIP. The critical stresses predicted for the various pavement sections utilized in the logistic calculations are presented in Table D-3. Surfacing weight, cost, and shipping volume for an airfield having a soil CBR value of 10% are tabulated in Table D-4.

*The C-130 which has an ESWL of 44,400 pounds is included because of its relatively low tire pressure of 95 psi.

**For the F-4, the width of traffic equals the lateral traffic distribution width plus the footprint width. The lateral traffic distribution width for nonchannelized traffic has been determined as 80 inch. The lateral traffic distribution width is the width within which the centerlines of all aircraft tend to remain 75% of the time in traveling along a pavement. The footprint width for the F-4E is 8.9 inches (Ref 22). Thus, the width of traffic for the F-4 is 88.9 inches (7.4 feet).

Table D-2. Design Aircraft Loads

Traffic Area	Critical Aircraft	Tire Pressure	Contact Area ($in.^2$)	Load Radius ($in.^2$)[a]	Rim Load[a]	
					Area ($in.^2$)	Pressure (psi)
A and C - Main Runway Shoulders and Medium Duty Parking Apron	F-4B	330.0	82.0	5.11	-	-
D - Main Runway Center[b]	F-4B	394.0	205.0	8.08	12.5	669
B - Light Duty Parking Apron	C-130	95.0	467.6	12.20	-	-

[a]Superposition of stresses calculated for tire load and rim load was used to determine pavement stresses from landing impact.

[b]Landing impact - 17 fps sink speed.

Table D-3. Predicted[a] Stresses for Soil CBR of 10

Traffic Area and Load	Pavement	Material[b]	Normal Stress			Shear Stress	
			σ_{max} (psi)	σ_{min} (psi)	Factor of Safety	τ_{max} (psi)	Factor of Safety
Area A, F-4B	AMSS 0.38 in.	FRP	3,120	-553	5.5	1,837	6.5
Area B, C-130	AMSS 0.25 in.	FRP	29	-340	43	176	68
Area C, F-4B	FIBERMAT 0.125/2.75, 20/10-1	FRP	-334	-3,585	4.7	1,626	7.4
		foam top	-238	-365	3.2	64	20.0
		foam bottom	792	-191	3.2	492	4.0
Area D, F-4B	FIBERMAT 0.25/3.25, 20/10-1	FRP	-916	-6,806	2.5	2,945	4.1
		foam top	-390	-1,084	1.1	347	3.6
		foam bottom	1,572	-364	1.6	968	2.0

[a]Boundary conditions of SLIP computer program:

(a) free to slip tangent to boundary and

(b) nodes at soil/surfacing interface locked in normal direction and unrestrained in tangent direction.

[b]Material Properties

FRP

$\sigma_{c(ULT)}$ = 17,000 psi

E_c = 1.5 x 10^6 psi

τ_{ULT} = 12,000 psi

ν = 0.25

Foam (10% Random Fibers)

$\sigma_{b(ULT)}$ = 1,600 psi

$\sigma_{c(ULT)}$ = 1,150 psi

E_b = 73,000 psi

τ_{ULT} = 1,250 psi

ν = 0.30

Foam (1 Layer 4020 Fiberglass)

$\sigma_{b(ULT)}$ = 2,500 psi

$\sigma_{c(ULT)}$ = 1,150 psi

E_b = 138,000 psi

τ_{ULT} = 1,950 psi

ν = 0.25

Soil

CBR = 10

E_s = 15,000 psi

ν = 0.30

Table D-4. EAF Logistics Summary for Soil CBR of 10[a]

[Average weight, 4.8 psf; average cost; $3.89/ft^2; cube ratio, 6.5 ft^2/ft^3]

Material Component	Density (lb/gal)	Materials by Traffic Area						Number of 8x8x20 Containers	Volume (ft^3)	Unit Cost, ($) 1980	Cost ($)
		B 382,736 ft^2 (lb)	A 461,928 ft^2 (lb)	C 264,000 ft^2 (lb)	D 114,000 ft^2 (lb)	C1 6,000 ft^2 (lb)	Totals (lb)				
Polyester Resin	10.2	665,730	1,205,215	212,165	183,233	10,503	2,276,846	74[b]	94,720	0.735	1,673,482
Fiberglass Cloth[c]	--	359,854	651,467	229,368	148,668	7,807	1,397,164	8[b,d]	10,240	0.875	1,222,519
Fiberglass Roving	--	--	--	122,210	62,410	2,761	187,381	5	6,400	0.690	129,293
Foam											
Component A	--	--	--	694,153	354,486	15,776	1,064,415	35	44,800	0.895	952,651
Component B	--	--	--	527,947	269,609	11,980	809,536	26	33,280	0.895	724,535
Solvent[e]	8.3	--	--	--	--	--	124,524	—[f]	--	0.375	46,697
Promoter	8.3	--	--	--	--	--	4,098	—[f]	--	3.730	15,286
Catalyst	8.3	--	--	--	--	--	16,393	—[f]	--	0.770	12,623
Totals	--	--	--	--	--	--	5,880,357	148	180,440		4,777,086

[a]The following allowances are included:
- o 0.74 psf polyester resin per layer (0.125 in.) of 4020 style fiberglass mat.
- o Resin and fiberglass quantities increased by 1% to account for waste.
- o Edge lapping of fiberglass mats by 6 in.

[b]Resin and fiberglass were considered to be packed together in 8 x 8 x 20-ft containers. Containers stuffed with 31,000 lb of resin plus 9,072 lb of fiberglass mat for a total payload of 40,072 lb. Resin packaged in modules within the container. Modules filled to 83% of their volume capacity.

[c]Weight equals 0.4 lb/ft^2 per layer.

[d]1,224,720 lb fiberglass packaged with polyester resin and foam components.

[e]Estimated at 3% solvent by weight of resins.

[f]Packaged with fiberglass mat.

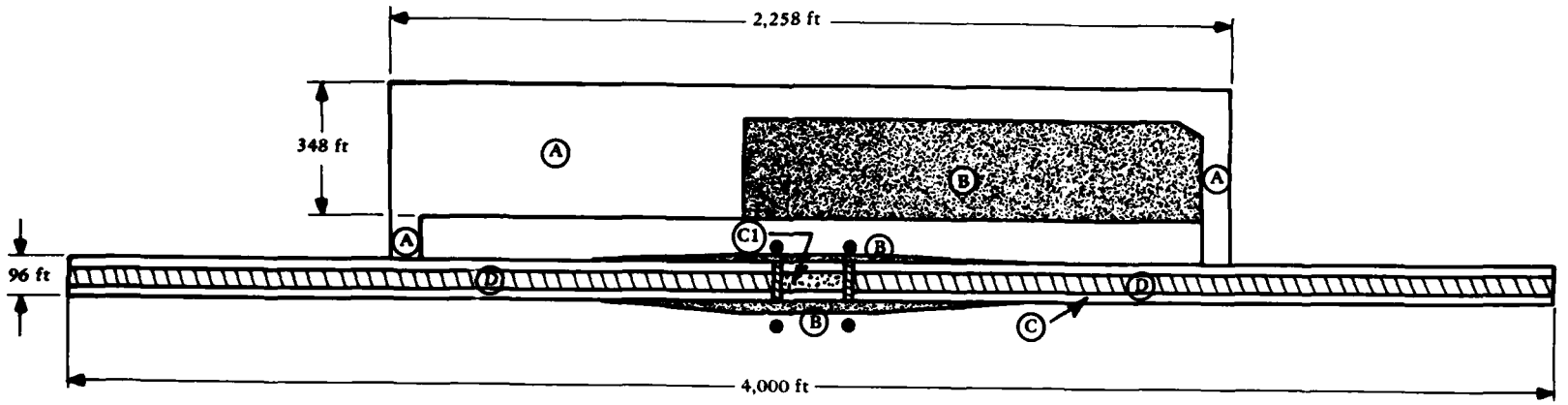

Note: Refer to Figure D-2 for runway detail. Surfacing area equals 1,228,664 ft^2.

Figure D-1. Expeditionary airfield traffic areas.

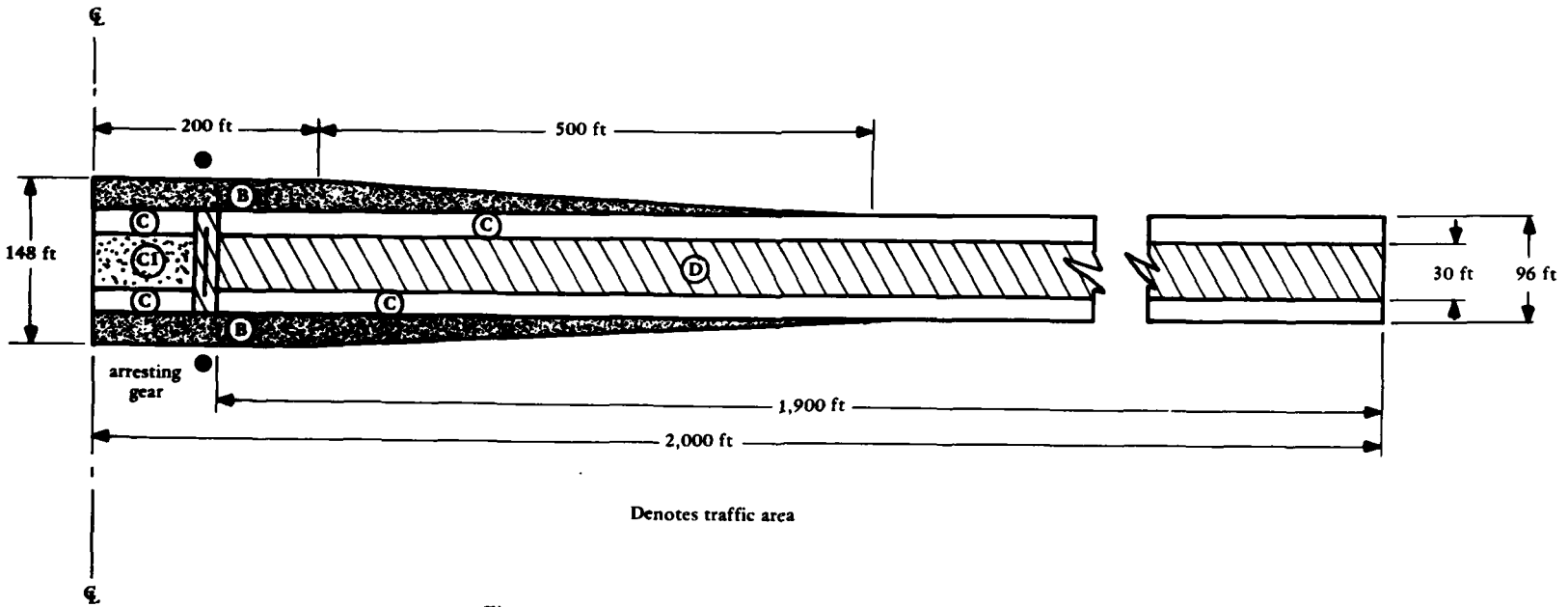

Figure D-2. Traffic areas for an Expeditionary Airfield runway.

DISTRIBUTION LIST

AF HQ PREES Washington DC (R P Reid)
AFB (AFIT/LD), Wright-Patterson OH; AF Tech Office (Mgt & Ops), Tyndall, FL; AFCEC/XR,Tyndall FL; CESCH, Wright-Patterson; HQ Tactical Air Cmd (R. E. Fisher), Langley AFB VA; HQAFESC/DEMM, Tyndall AFB, FL; MAC/DET (Col. P. Thompson) Scott, IL; SAMSO/MNND, Norton AFB CA; Stinfo Library, Offutt NE
ARMY ARRADCOM, Dover, NJ; BMDSC-RE (H. McClellan) Huntsville AL; DAEN-MCE-D (R L Wight) Washington DC; DAEN-MPE-D Washington DC; ERADCOM Tech Supp Dir. (DELSD-L) Ft. Monmouth, NJ; HQ-DAEN-MPO-B (Mr. Price); Tech. Ref. Div., Fort Huachuca, AZ
ARMY - CERL Library, Champaign IL
ARMY COE Philadelphia Dist. (LIBRARY) Philadelphia, PA
ARMY CORPS OF ENGINEERS MRD-Eng. Div., Omaha NE; Seattle Dist. Library, Seattle WA
ARMY CRREL R.A. Eaton
ARMY DARCOM AMCPM-CS (J. Carr), Alexandria VA
ARMY ENG DIV ED-CS (S.Bolin) Huntsville, AL; HNDED-CS, Huntsville AL; HNDED-SR, Huntsville, AL
ARMY ENG WATERWAYS EXP STA Library, Vicksburg MS
ARMY ENVIRON. HYGIENE AGCY B620, Edgewood Arsenal MD; Water Qual Div (Doner), Aberdeen Prov Ground, MD
ARMY MATERIALS & MECHANICS RESEARCH CENTER Dr. Lenoe, Watertown MA
ARMY MISSILE R&D CMD Redstone Arsenal AL Sci. Info. Cen (Documents)
ARMY TRANSPORTATION SCHOOL MAJ T Sweeney, Code ATSP CD-TE Fort Eustis VA
ASST SECRETARY OF THE NAVY Spec. Assist Energy (Leonard), Washington, DC
CINCLANT Civil Engr. Supp. Plans. Ofr Norfolk, VA
CINCPAC Fac Engrng Div (J44) Makalapa, HI
CNO Code NOP-964, Washington DC; OP987J (J. Boosman), Pentagon
COMCBPAC Operations Off, Makalapa HI
COMFAIRWESTPAC Security Offr, Misawa Japan
COMNAVBEACHPHIBREFTRAGRU ONE San Diego CA
COMNAVMARIANAS Code N4, Guam
COMOCEANSYSPAC SCE, Pearl Harbor HI
COMSUBDEVGRUONE Operations Offr, San Diego, CA
DEFENSE CIVIL PREPAREDNESS AGENCY J.O. Buchanan, Washington DC
DEFENSE INTELLIGENCE AGENCY Dir., Washington DC
DLSIE Army Logistics Mgt Center, Fort Lee, VA
DNA STTL, Washington DC
DOD Explosives Safety Board (Library), Washington DC
DOE Dr. Cohen
DTNSRDC Code 1706, Bethesda MD
DTNSRDC Code 4121 (R. Rivers), Annapolis, MD
FLTCOMBATTRACENLANT PWO, Virginia Bch VA
FMFLANT CEC Offr, Norfolk VA
MARINE CORPS BASE Camp Pendleton CA 92055; Code 43-260, Camp Lejeune NC; M & R Division, Camp Lejeune NC; PWO Camp Lejeune NC; PWO, Camp S. D. Butler, Kawasaki Japan
MARINE CORPS HQS Code LFF-2, Washington DC
MCAS Facil. Engr. Div. Cherry Point NC; Code PWE, Kaneohe Bay HI; Code S4, Quantico VA; PWO Kaneohe Bay HI; PWO, Yuma AZ; SCE, Futema Japan
MCDEC NSAP REP, Quantico VA; P&S Div Quantico VA
MCLSBPAC PWO, Barstow CA
NAF PWD - Engr Div, Atsugi, Japan; PWO Sigonella Sicily; PWO, Atsugi Japan
NAS CO, Guantanamo Bay Cuba; Code 114, Alameda CA; Code 183 (Fac. Plan BR MGR); Code 18700, Brunswick ME; Code 18U (ENS P.J. Hickey), Corpus Christi TX; Code 6234 (G. Trask), Point Mugu CA; Code 70, Atlanta, Marietta GA; Dir. Maint. Control Div., Key West FL; Dir. Util. Div., Bermuda; ENS Buchholz, Pensacola, FL; Lakehurst, NJ; PW (J. Maguire), Corpus Christi TX; PWD Maint. Cont. Dir., Fallon NV; PWD Maint. Div., New Orleans, Belle Chasse LA; PWD, Maintenance Control Dir., Bermuda; PWD, Willow Grove PA; PWO Belle Chasse, LA; PWO Chase Field Beeville, TX; PWO Key West FL;

PWO Whiting Fld, Milton FL; PWO, Dallas TX; PWO, Glenview IL; PWO, Kingsville TX; PWO, Millington TN; PWO, Miramar, San Diego CA; PWO., Moffett Field CA; ROICC Key West FL; SCE Lant Fleet Norfolk, VA; SCE Norfolk, VA; SCE, Barbers Point HI; Security Offr, Alameda CA

NATL RESEARCH COUNCIL Naval Studies Board, Washington DC

NAVACT PWO, London UK

NAVAEROSPREGMEDCEN SCE, Pensacola FL

NAVCOASTSYSCEN Code 772 (C B Koesy) Panama City FL

NAVCOASTSYSTCTR Code 713 (J. Quirk) Panama City, FL; Library Panama City, FL

NAVCOMMAREAMSTRSTA PWO, Norfolk VA; PWO, Wahiawa HI; SCE Unit 1 Naples Italy

NAVCOMMSTA Code 401 Nea Makri, Greece; PWO, Exmouth, Australia

NAVEDTRAPRODEVCEN Tech. Library

NAVEDUTRACEN Engr Dept (Code 42) Newport, RI

NAVEODFAC Code 605, Indian Head MD

NAVFAC PWO, Centerville Bch, Ferndale CA

NAVFAC PWO, Lewes DE

NAVFACENGCOM Code 043 Alexandria, VA; Code 044 Alexandria, VA; Code 0451 Alexandria, VA; Code 0454B Alexandria, Va; Code 04B5 Alexandria, VA; Code 100 Alexandria, VA; Code 1002B (J. Leimanis) Alexandria, VA; Code 1113 (T. Stevens) Alexandria, VA; Code 1113 Alexandria, VA; Morrison Yap, Caroline Is.; P W Brewer Alexandria, VA

NAVFACENGCOM - CHES DIV, Code 101 Wash, DC; Code 102, (Wildman), Wash, DC; Code 405 Wash, DC; Code FPO-1 Wash, DC

NAVFACENGCOM - LANT DIV, Code 405, Norfolk, VA; Eur. BR Deputy Dir, Naples Italy; European Branch, New York; RDT&ELO 102, Norfolk VA

NAVFACENGCOM - NORTH DIV, CO; Code 09P (LCDR A.J. Stewart); Code 102; Code 1028, RDT&ELO, Philadelphia PA; Design Div, (R. Masino), Philadelphia PA; ROICC, Contracts, Crane IN

NAVFACENGCOM - PAC DIV, (Kyi) Code 101, Pearl Harbor, HI; Code 2011 Pearl Harbor, HI; Code 402, RDT&E, Pearl Harbor HI; Commander, Pearl Harbor, HI

NAVFACENGCOM - SOUTH DIV, Code 405, RDT&ELO, Charleston, SC; Code 90, RDT&ELO, Charleston SC

NAVFACENGCOM - WEST DIV, 102; Code 04B San Bruno, CA; O9P/20 San Bruno, CA; RDT&ELO Code 2011 San Bruno, CA

NAVFACENGCOM CONTRACT AROICC, Point Mugu CA; AROICC, Quantico, VA; Eng Div dir, Southwest Pac, Manila, PI; OICC, Southwest Pac, Manila, PI; OICC/ROICC, Balboa Canal Zone; ROICC AF Guam; ROICC LANT DIV., Norfolk VA; ROICC, Keflavik, Iceland; ROICC, Pacific, San Bruno CA

NAVHOSP LT R. Elsbernd, Puerto Rico

NAVMAG SCE, Guam

NAVOCEANSYSCEN Research Lib., San Diego CA

NAVPETOFF Code 30, Alexandria VA

NAVPGSCOL Code 61WL (O. Wilson) Monterey CA

NAVPHIBASE CO, ACB 2 Norfolk, VA; Code S3T, Norfolk VA

NAVREGMEDCEN Code 29, Env. Health Serv, (Al Bryson) San Diego, CA; SCE (D. Kaye); SCE, Camp Pendleton CA; SCE, Oakland CA

NAVSCOLCECOFF C35 Port Hueneme, CA

NAVSEASYSCOM Code 0325, Program Mgr, Washington, DC

NAVSEC Code 6034 (Library), Washington DC

NAVSECGRUACT PWO, Adak AK; PWO, Torri Sta, Okinawa

NAVSHIPYD; Code 202.4, Long Beach CA; Code 202.5 (Library) Puget Sound, Bremerton WA; Code 404 (LT J. Riccio), Norfolk, Portsmouth VA; Code 410, Mare Is., Vallejo CA; Code 440 Portsmouth NH; Code 440, Puget Sound, Bremerton WA; Library, Portsmouth NH; Tech Library, Vallejo, CA

NAVSTA CO Naval Station, Mayport FL; CO Roosevelt Roads P.R. Puerto Rico; Maint. Div. Dir/Code 531, Rodman Canal Zone; PWD (LTJG.P.M. Motolenich), Puerto Rico; PWO, Guantanamo Bay Cuba; PWO, Keflavik Iceland; PWO, Mayport FL; SCE, Guam; SCE, San Diego CA; SCE, Subic Bay, R.P.; Utilities Engr Off. (A.S. Ritchie), Rota Spain

NAVSUPPACT CO, Seattle WA; LTJG McGarrah, SEC, Vallejo, CA

NAVSURFWPNCEN PWO, White Oak, Silver Spring, MD

NAVTECHTRACEN SCE, Pensacola FL

NAVWPNCEN Code 2636 (W. Bonner), China Lake CA; PWO (Code 26), China Lake CA; ROICC (Code 702), China Lake CA

NAVWPNSTA Maint. Control Dir., Yorktown VA
NAVWPNSTA PW Office (Code 09C1) Yorktown, VA
NAVWPNSTA PWO, Seal Beach CA; Security Offr, Colts Neck NJ
NAVWPNSUPPCEN Code 09 Crane, IN
NCBU 405 OIC, San Diego, CA
NCBC CEL AOIC Port Hueneme CA; Code 10 Davisville, RI; Code 155, Port Hueneme CA; Code 156, Port Hueneme, CA; Code 400, Gulfport MS; PWO, Davisville RI
NCR 20, Commander
NMCB 5, Operations Dept.; 74, CO; Forty, CO; THREE, Operations Off.
NORDA Code 440 (Ocean Rsch Off) Bay St. Louis MS
NRL Code 8400 Washington, DC; Code 8441 (R.A. Skop), Washington DC
NSC Code 54.1 (Wynne), Norfolk VA
NSD SCE, Subic Bay, R.P.
NTC Commander Orlando, FL; OICC, CBU-401, Great Lakes IL
NUSC Code 131 New London, CT; Code EA123 (R.S. Munn), New London CT
ONR Code 700F Arlington VA; Dr. A. Laufer, Pasadena CA
PACMISRANFAC CO, Kekaha HI
PHIBCB 1 P&E, Coronado, CA
PMTC Pat. Counsel, Point Mugu CA
PWC CO Norfolk, VA; CO, (Code 10), Oakland, CA; CO, Great Lakes IL; Code 10, Great Lakes, IL; Code 120, Oakland CA; Code 120C, (Library) San Diego, CA; Code 128, Guam; Code 154, Great Lakes, IL; Code 200, Guam; Code 220 Oakland, CA; Code 220.1, Norfolk VA; Code 30C, San Diego, CA; Code 400, Great Lakes, IL; Code 400, Oakland, CA; Code 400, Pearl Harbor, HI; Code 400, San Diego, CA; Code 420, Great Lakes, IL; Code 420, Oakland, CA; Code 600, Great Lakes, IL; Code 610, San Diego Ca; Code 700, Great Lakes, IL; Code 700, San Diego, CA; LTJG J.L. McClaine, Yokosuka, Japan; Library, Subic Bay, R.P.; Utilities Officer, Guam; XO (Code 20) Oakland, CA
NAF PWO (Code 30) El Centro, CA
U.S. MERCHANT MARINE ACADEMY Kings Point, NY (Reprint Custodian)
US NAVAL FORCES Korea (ENJ-P&O)
USCG G-EOE-4/61 (T. Dowd), Washington DC
USDA Forest Service, Bowers, Atlanta, GA; Forest Service, San Dimas, CA
USEUCOM (ECJ4/L-LO), Wright, Stuttgart, GE
USNA Ch. Mech. Engr. Dept Annapolis MD; PWD Engr. Div. (C. Bradford) Annapolis MD
CALIFORNIA STATE UNIVERSITY LONG BEACH, CA (CHELAPATI)
CORNELL UNIVERSITY Ithaca NY (Serials Dept, Engr Lib.)
DAMES & MOORE LIBRARY LOS ANGELES, CA
IOWA STATE UNIVERSITY Ames IA (CE Dept, Handy)
LEHIGH UNIVERSITY Bethlehem PA (Fritz Engr. Lab No. 13, Beedle); Bethlehem PA (Linderman Lib. No.30, Fleeksteiner)
LIBRARY OF CONGRESS WASHINGTON, DC (SCIENCES & TECH DIV)
MICHIGAN TECHNOLOGICAL UNIVERSITY Houghton, MI (Haas)
MIT Cambridge MA; Cambridge MA (Rm 10-500, Tech. Reports, Engr. Lib.); Cambridge MA (Whitman)
NY CITY COMMUNITY COLLEGE BROOKLYN, NY (LIBRARY)
OREGON STATE UNIVERSITY CORVALLIS, OR (CE DEPT, BELL); CORVALLIS, OR (CE DEPT, HICKS)
PURDUE UNIVERSITY Lafayette IN (Leonards); Lafayette, IN (Altschaeffl); Lafayette, IN (CE Engr. Lib)
SEATTLE U Prof Schwaegler Seattle WA
SOUTHWEST RSCH INST R. DeHart, San Antonio TX
STANFORD UNIVERSITY Engr Lib, Stanford CA
STATE UNIV. OF NEW YORK Buffalo, NY
TEXAS A&M UNIVERSITY W.B. Ledbetter College Station, TX
UNIVERSITY OF CALIFORNIA BERKELEY, CA (CE DEPT, GERWICK); BERKELEY, CA (CE DEPT, MITCHELL); DAVIS, CA (CE DEPT, TAYLOR); LIVERMORE, CA (LAWRENCE LIVERMORE LAB, TOKARZ)
UNIVERSITY OF HAWAII Honolulu HI (Dr. Szilard)
UNIVERSITY OF ILLINOIS Metz Ref Rm, Urbana IL; URBANA, IL (LIBRARY); URBANA, IL (NEWMARK); Urbana IL (CE Dept, W. Gamble)
UNIVERSITY OF MASSACHUSETTS (Heronemus), Amherst MA CE Dept

UNIVERSITY OF MICHIGAN Ann Arbor MI (Richart)
UNIVERSITY OF NEBRASKA-LINCOLN Lincoln, NE (Ross Ice Shelf Proj.)
UNIVERSITY OF NEW MEXICO J Nielson-Engr Matls & Civil Sys Div, Albuquerque NM
UNIVERSITY OF NOTRE DAME Katona, Notre Dame, IN
UNIVERSITY OF TEXAS Inst. Marine Sci (Library), Port Arkansas TX
UNIVERSITY OF TEXAS AT AUSTIN AUSTIN, TX (THOMPSON); Austin, TX (Breen)
UNIVERSITY OF WASHINGTON Dept of Civil Engr (Dr. Mattock), Seattle WA; SEATTLE, WA (MERCHANT); Seattle, WA Transportation, Construction & Geom. Div
URS RESEARCH CO. LIBRARY SAN MATEO, CA
AMETEK Offshore Res. & Engr Div
ARVID GRANT OLYMPIA, WA
ATLANTIC RICHFIELD CO. DALLAS, TX (SMITH)
BECHTEL CORP. SAN FRANCISCO, CA (PHELPS)
BELGIUM HAECON, N.V., Gent
BROWN & CALDWELL E M Saunders Walnut Creek, CA
CANADA Mem Univ Newfoundland (Chari), St Johns; Surveyor, Nenninger & Chenevert Inc., Montreal; Trans-Mnt Oil Pipe Lone Corp. Vancouver, BC Canada
FRANCE Dr. Dutertre, Boulogne
GLIDDEN CO. STRONGSVILLE, OH (RSCH LIB)
HALEY & ALDRICH, INC. Cambridge MA (Aldrich, Jr.)
HUGHES AIRCRAFT Culver City CA (Tech. Doc. Ctr)
ITALY M. Caironi, Milan
MC CLELLAND ENGINEERS INC Houston TX (B. McClelland)
MCDONNEL AIRCRAFT CO. Dept 501 (R.H. Fayman), St Louis MO
NEWPORT NEWS SHIPBLDG & DRYDOCK CO. Newport News VA (Tech. Lib.)
NORWAY DET NORSKE VERITAS (Library), Oslo; DET NORSKE VERITAS (Roren) Oslo; I. Foss, Oslo; J. Creed, Ski; Norwegian Tech Univ (Brandtzaeg), Trondheim
PORTLAND CEMENT ASSOC. SKOKIE, IL (CORLEY; Skokie IL (Rsch & Dev Lab, Lib.)
RAND CORP. Santa Monica CA (A. Laupa)
RAYMOND INTERNATIONAL INC. E Colle Soil Tech Dept, Pennsauken, NJ
SANDIA LABORATORIES Library Div., Livermore CA
SCHUPACK ASSOC SO. NORWALK, CT (SCHUPACK)
SHELL OIL CO. HOUSTON, TX (MARSHALL)
SWEDEN Cement & Concrete Research Inst., Stockholm; GeoTech Inst
TIDEWATER CONSTR. CO Norfolk VA (Fowler)
TRW SYSTEMS REDONDO BEACH, CA (DAI)
UNITED KINGDOM Cement & Concrete Assoc Wexham Springs, Slough Bucks; Cement & Concrete Assoc. (Lit. Ex), Bucks; D. Lee, London; D. New, G. Maunsell & Partners, London; R. Browne, Southall, Middlesex; Taylor, Woodrow Constr (014P), Southall, Middlesex
WESTINGHOUSE ELECTRIC CORP. Annapolis MD (Oceanic Div Lib, Bryan); Library, Pittsburgh PA
WISS, JANNEY, ELSTNER, & ASSOC Northbrook, IL (D.W. Pfeifer)
WOODWARD-CLYDE CONSULTANTS (A. Harrigan) San Francisco
BROWN, ROBERT University, AL
BULLOCK La Canada
ERVIN, DOUG Belmont, CA
F. HEUZE Alamo, CA
CAPT MURPHY Sunnyvale, CA
R.F. BESIER Old Saybrook CT